

Radial-velocity survey of members and candidate members of the TW Hydrae association¹

** To appear in the February 2003 issue of The Astronomical Journal **

Guillermo Torres², Eike W. Guenther³, Laurence A. Marschall⁴, Ralph Neuhauser⁵, David W. Latham², Robert P. Stefanik²

gtorres@cfa.harvard.edu

ABSTRACT

We report our spectroscopic observations of stars belonging to the young nearby group known as the TW Hydrae association, as well as of a number of potential members of the association identified in kinematic and X-ray surveys. Multiple radial velocity measurements were obtained for each object, several of which turn out to be multiple systems. Orbital solutions are presented for 3 double-lined binaries, one single-lined binary, and a double-lined triple system, all with short periods. Effective temperatures and projected rotational velocities are presented for each visible object. None of the candidate members of the association in our sample is confirmed as a true member. The large fraction of close binaries among the candidate members has to do with their selection based on X-ray emission from ROSAT, which tends to favor the inclusion of tidally-locked systems that are active but not necessarily young.

Subject headings: stars: pre-main sequence — stars: kinematics — binaries: spectroscopic — open clusters and associations: individual (TW Hydrae)

¹Some of the observations reported here were obtained with the Multiple Mirror Telescope, a joint facility of the Smithsonian Institution and the University of Arizona.

²Harvard-Smithsonian Center for Astrophysics, 60 Garden St., Cambridge, MA 02138

³Thüringer Landessternwarte Tautenburg, Karl-Schwarzschild-Observatorium, Sternwarte 5, 07778 Tautenburg, Germany

⁴Department of Physics, Gettysburg College, 300 North Washington Street, Gettysburg, PA 17325

⁵Max-Planck-Institut für extraterrestrische Physik, D-85740 Garching, Germany

1. Introduction

In recent years a number of loose associations of nearby stars have been identified that appear to be very young, yet show no signs of molecular gas in the surroundings —one of the more visible characteristics of the classical regions of star formation. Among these new groups are the TW Hydrae association (Kastner et al. 1997), the η Chamaeleontis cluster (Mamajek, Lawson & Feigelson 1999), the Tucana association (Zuckerman & Webb 2000), the Horologium association (Torres et al. 2000) (which may be the same or related to the latter; Zuckerman 2001; Guenther et al. 2001), the Capricornius association or HD 199143 group (van den Ancker, Pérez & de Winter 2001), which is probably related or is a subgroup of the β Pictoris group (Zuckerman et al. 2001a), and others. Other small groups are similarly young and nearby but do appear to be associated with gas, such as the stars in the high-latitude MBM12 cloud (Hearty et al. 2000a,b). The distances to these groups are in the range from ~ 35 to ~ 150 pc, and they all seem to have similar ages around 10 Myr. The fact that most of them are in the southern sky is probably not a coincidence, and may be related to their association with the Gould Belt, or more specifically, the Sco-Cen association and its subgroups (see Mamajek, Lawson & Feigelson 2000; Mamajek & Feigelson 2001).

The best known of these small groups of young stars is the TW Hya association, named after the first classical T Tauri star found in isolation from any known cloud material (Henize 1976; Herbig 1978; Rucinski & Krautter 1983). Surveys by de la Reza et al. (1989) and Gregorio-Hetem et al. (1992) based on the IRAS Point-Source Catalog turned up four other T Tauri stars in the same region of the sky, and the physical association between all these stars was suggested by Kastner et al. (1997) on the basis of the similarity of their optical as well as their X-ray properties. Subsequent systematic searches revealed other apparently related stars, after it was found that they also appear to share a similar space velocity. A few previously known young stars in the same area of the sky with similar characteristics were also included in the group. To date there are some 20 recognized members spread over hundreds of square degrees (Kastner et al. 1997; Webb et al. 1999; Sterzik et al. 1999; Zuckerman et al. 2001b), along with a number of other candidate members identified on the basis of their kinematics, their X-ray properties, or their infrared (2MASS) colors and spectral features (see, e.g., Gizis 2002). The typical distance of these objects is roughly 60 pc, although there appears to be a significant spread.

Many of them have been the subject of a broad range of studies to characterize their properties and to establish their youth, by measuring the strength of their H α emission, Li I $\lambda 6708$ absorption, infrared excess, etc. Other high-resolution imaging investigations have focussed on circumstellar disks (TW Hya, HR 4796A, Hen 3-600A, HD 98800B) and binary companions, and have even revealed the presence of a probable brown dwarf around

one of the stars (CD–33°7795; Lowrance, McCarthy & Becklin 1999; Webb et al. 1999; Neuhäuser et al. 2000a).

Kinematic investigations relying on the assumption of a common space motion for the members of the TW Hya association (convergent point solution) have been carried out by Makarov & Fabricius (2001) and also Frink (2001) to study the structure of the group, using the proper motions of the known members and trigonometric parallaxes from the HIPPARCOS mission for the few stars that have them. In this way additional members have been proposed, and radial velocities have been predicted for the known and candidate stars by Makarov & Fabricius (2001). Direct measurements of the radial velocities of these stars have been made rather sparingly over the past few years by a number of authors, and occasional discrepancies have shown up. Observations for most of these new candidates have been reported recently by Song, Bessell & Zuckerman (2002). Essentially all of these studies are based on a single measurement of the velocity of each star or on observations over a very limited time interval, rather than on a systematic monitoring over time. Since some of the objects may be binaries, this could explain some of the differences mentioned above.

In this paper we present the results of our radial-velocity monitoring of members and candidate members of the TW Hya association over the past several years, with multiple observations per object. This has allowed us to solve for the spectroscopic orbits of several binaries as well as one triple system, and to determine the physical properties (effective temperature, projected rotational velocity) of all visible components. A preliminary report of this work was given by Torres, Neuhäuser & Latham (2001), and the full details based on additional observations are given here.

2. Sample and observations

Potential members of the TW Hya association were drawn from reports by Hoff, Alcalá & Sterzik (1997), Hoff, Henning & Pfau (1998), Sterzik et al. (1999), and Makarov & Fabricius (2001), and a few other objects were added on the basis of their proximity to the known members and the similarity of their X-ray properties from ROSAT. In addition, 7 known members were also observed, including their binary companions when possible. Table 1 lists the optical properties of the stars in our sample. Conventional designations in the association (e.g., TWA-1) are given in column (2), and other columns present alternate designations, coordinates, visual magnitudes, spectral types, and Li I $\lambda 6708$ equivalent widths. We have included in this list the quadruple system HD 98800 (TWA-4) for completeness, given that it was observed several years ago with the same instrumental setup described below (Torres et al. 1995). The X-ray properties of these stars are given in Table 2. They

include ROSAT positions and their uncertainty (close binaries are unresolved), the Maximum Likelihood estimator ML that provides a measure of the existence of the source above the local background (Cruddace, Hasinger & Schmitt 1988), the exposure time and count rate, and the X-ray hardness ratios (see Neuhäuser et al. 1995). These data are taken from the ROSAT All-Sky Survey Catalog 1RXS (Voges et al. 1999)⁶. The majority of the spectroscopic observations for the present investigation were obtained with various telescopes at the Harvard-Smithsonian Center for Astrophysics (CfA), and a few also at the 1.5-m ESO telescope at La Silla (Chile) and the 2-m telescope in Tautenburg (Germany).

Observations at the CfA were made using nearly identical echelle spectrographs on the 1.5-m Wyeth reflector at the Oak Ridge Observatory (Harvard, Massachusetts), the 1.5-m Tillinghast reflector at the F. L. Whipple Observatory (Mt. Hopkins, Arizona) and the Multiple Mirror Telescope (also on Mt. Hopkins, Arizona) prior to its conversion to a monolithic 6.5-m mirror. A single echelle order was recorded with photon-counting intensified Reticon detectors at a central wavelength of 5187 Å, with a spectral coverage of 45 Å. The resolving power is $\lambda/\Delta\lambda \approx 35,000$, and the signal-to-noise (S/N) ratios achieved range from about 7 to 50 per resolution element of 8.5 km s⁻¹. A total of 509 spectra were collected over a period of 18 years (1984–2002), including archival observations of similar quality for some of the objects that were observed with the same instruments prior to the start of this project.

Radial velocities were obtained using the cross-correlation task XCSAO (Kurtz & Mink 1998) running under IRAF⁷. Typical uncertainties for an individual measurement are smaller than 1 km s⁻¹. For stars with temperatures hotter than ~ 4000 K we used templates from a grid of synthetic spectra computed for us by Jon Morse, based on the latest model atmospheres by R. L. Kurucz⁸ (see Nordström et al. 1994). These calculated spectra are available for a wide range of effective temperatures (T_{eff}), projected rotational velocities ($v \sin i$), surface gravities ($\log g$) and metallicities. The optimum template for each object was determined from extensive grids of correlations in temperature and rotational velocity (the two parameters that affect the radial velocities the most), for an adopted surface gravity and for solar metallicity. We adopted for the stellar properties the parameters giving the highest correlation averaged over all exposures, interpolated between neighboring templates for higher accuracy. The errors for the effective temperature and $v \sin i$ determinations are

⁶The catalog and updates are available at <http://www.xray.mpe.mpg.de/rosat/survey/rass-bsc/>.

⁷IRAF is distributed by the National Optical Astronomy Observatories, which is operated by the Association of Universities for Research in Astronomy, Inc., under contract with the National Science Foundation.

⁸Available at <http://cfaku5.harvard.edu>.

estimated to be around 150 K and 2–3 km s⁻¹, respectively, unless noted otherwise. For objects cooler than about 4000 K the synthetic templates become less realistic because they lack several key molecular opacity sources. In those cases we used observed templates from strong exposures of late-type stars.

Several of our objects turned out to have composite spectra (two sets of lines present). For those we determined the radial velocities using TODCOR (Zucker & Mazeh 1994), which is a two-dimensional cross-correlation technique well suited to our relatively low S/N observations. Grids of correlations analogous to those described above were run to determine the stellar properties for both components, whenever possible. The temperature and $v \sin i$ determinations for all visible objects are given in Table 3, and are compared with similar determinations by other authors. The agreement in most cases is reasonably good.

The stability of the zero-point of the CfA velocity system was monitored by means of exposures of the dusk and dawn sky, and small systematic run-to-run corrections were applied in the manner described by Latham (1992). The zero point of the native CfA velocity system based on synthetic templates is very close to the absolute frame as defined by extensive observations of the minor planets in the solar system. The correction required to place our radial velocities on this absolute frame is +0.139 km s⁻¹ (Stefanik, Latham & Torres 1999; Latham et al. 2002).

Forty-two additional observations for four of the objects were obtained with the echelle spectrograph FEROS (Fiber-fed Extended Range Optical Spectrograph) on the 1.5-m ESO telescope at La Silla. The wavelength coverage is approximately from 3600 Å to 9200 Å (38 echelle orders), and the resolving power is $\lambda/\Delta\lambda \approx 48,000$. Due to the relative faintness of the stars the observations were carried out in ‘object+sky’ mode rather than in the mode in which calibrations are taken simultaneously with the object. We obtained 3 spectra of TWA-1 (TW Hya), 3 of TWA-2A (CD–29°8887A), 18 of TWA-3A (Hen 3-600A), and 18 spectra of TWA-5A (CD–33°7795A). The S/N ratios for these observations range from 40 to 70 per 0.03 Å pixel at $\lambda 6708$. The standard MIDAS pipeline for FEROS was used to subtract the bias, flat-field, remove the scattered light, subtract the sky background, and to extract and wavelength-calibrate the spectra. Telluric lines were used to determine the instrumental shift between the observed spectra and the Th-Ar comparison spectra taken at the beginning and at the end of each night. Radial velocities were determined by measuring the position of photospheric lines in the spectra, and then applying the instrumental shift along with the barycentric correction. Tests showed that the error of the radial velocities derived in this way is approximately 0.3–0.4 km s⁻¹.

An additional spectrum of HIP 53486 was taken with the Coudé echelle spectrograph on the 2-m Alfred Jensch telescope in Tautenburg (Germany). Use of a 1"2 slit yielded a

resolution of $\lambda/\Delta\lambda \approx 67,000$, and the wavelength region covered is 4680–7400 Å. Standard IRAF routines were used to flat-field and extract the spectra. Th-Ar comparison lamp spectra at the beginning and end of the night were used to establish the wavelength reference, and instrumental shifts were determined using telluric lines.

In addition to the radial velocity determinations we also measured the strength of the Li I $\lambda 6708$ absorption line from the FEROS and Tautenburg spectra. This is one of the classical indicators of stellar youth (see, e.g., Bodenheimer 1965; Skumanich 1972). Our equivalent width measurements are 0.455 ± 0.016 Å for TWA-1, 0.560 ± 0.010 Å for TWA-2A, 0.658 ± 0.020 Å for TWA-5A, and an upper limit of 0.02 Å for HIP 53486. These have been combined with other measurements from the literature and listed as averages in Table 1.

3. Stars with orbital solutions

Multi-epoch observations for a number of our objects revealed obvious velocity variations, or double or distorted peaks in the correlation functions indicating the presence of a companion. Radial velocities for each component were measured whenever possible. In several cases we were able to derive spectroscopic orbital solutions, which we describe here separately for each system. None of these objects turn out to be true members of the TW Hya association, with the exception of the previously known case of TWA-4 A/B (HD 98800 A/B). Two other stars that are clearly multiple have so far defied all our attempts to establish the orbits, but will continue to be observed to that end and will be the subject of a future paper. They are TWA-3A (Hen 3-600A) and TWA-5A (CD–33°7795A), which are bona-fide members of the association and have been recognized previously by other authors as being spectroscopic binaries (Webb et al. 1999; Muzerolle et al. 2000; Torres et al. 2000). Both cases are complicated by the presence of visual companions. The secondary of TWA-3A (TWA-3B) is at a separation of $1''.44$ and has a magnitude difference of $\Delta V \sim 0.5$ mag. The close visual companion of TWA-5A was recently discovered using adaptive optics at a separation of only $0''.06$ (Macintosh et al. 2001) and a nearly equal brightness as the primary, and is different from the very faint TWA-5B (separation $\sim 2''$), and possibly different also from the spectroscopic companion. A brief discussion of each of our orbital solutions follows.

3.1. HIP 48273

This object (also known as 4 Sex, HD 85217, and HR 3893) was proposed as a possible member of the TW Hya association by Makarov & Fabricius (2001), although they concluded

from its kinematics that it is most likely not a true member. Double lines revealing the binary nature of the star were originally discovered by Shajn (1932), and preliminary orbital solutions were published by Popper & Shajn (1948), Popper (1949), and Mayor & Mazeh (1987), with a period of 3.05 d and an insignificant eccentricity. Systematic trends in the residuals of the orbit over the 16-yr interval of observation were reported by Popper & Shajn (1948), suggesting the possible presence of another star in the system. However, our higher quality solution based on nearly twice as many observations over a comparable period of time shows no such trend. Mayor & Mazeh (1987) reported a significant decrease in the velocity semiamplitudes K_A and K_B from a comparison between their orbit and that of Popper & Shajn (1948), which is based on observations obtained some 42 yr earlier. They interpreted this change as an indication that there is a third star in the system, which causes a precession of the node of the orbit of the binary that results in a slow and periodic change in the inclination angle. Our long coverage with virtually no change in the instrumental setup allows us to examine this claim by dividing our observations into two independent data sets, with a difference in the mean epochs of ~ 10 yr. No significant differences are seen in the velocity amplitudes, despite our uncertainties in the K values being much smaller than previous solutions.

Table 4 lists our radial-velocity measurements, and Table 5 gives the elements of the orbital solution. The orbit is circular. The fit is displayed in Figure 1.

From the short orbital period one may assume that the components’ rotation is synchronized with the orbital motion and their spin axes are parallel to the axis of the orbit. The system is then detached, and the minimum inclination angle for eclipses to occur is $i_{\min} \approx 77^\circ$ (see Torres, Neuhäuser & Guenther 2002). Assuming normal masses for stars of the temperatures we determine (e.g., based on the tabulation by Gray 1992), the actual inclination angle must be close to i_{\min} . However, no eclipses are seen in the epoch photometry provided by the HIPPARCOS mission, which displays a scatter of only 7 millimagnitudes⁹.

The light ratio between the primary and secondary at the wavelength of our observations (5187 Å) is $l_B/l_A = 0.66 \pm 0.02$. The mass ratio and the light ratio are consistent with the mass-luminosity relation for main-sequence stars. This, along with the weak Li I $\lambda 6708$ absorption (even correcting for duplicity) indicates the system is probably not in the pre-main sequence stage, and therefore is unlikely to be a true member of the association. The center-of-mass velocity of $+16.3 \text{ km s}^{-1}$ is also quite different from the typical value of about

⁹Two of the HIPPARCOS observations show a brightness ~ 0.15 mag fainter than the average, and happen to occur at phases 0.282 and 0.726, very near the predicted times of eclipse at phase 0.25 and 0.75. Although this would appear to suggest perhaps grazing eclipses, other observations at similar phases show the object at normal brightness, indicating that the low points are probably due to measurement errors.

+11 km s⁻¹ for true members (see §5).

3.2. TYC 6604-0118-1

This soft X-ray source from the Einstein Observatory Extended Medium Sensitivity Survey (Gioia et al. 1990; Stocke et al. 1991), referred to there as 1E0956.8–2225, was also proposed as a possible member of the TW Hya association by Makarov & Fabricius (2001). It was originally identified as a possible spectroscopic binary by Fleming (1988), and is also known by the names SAO 178272 and BD–21°2961, among others. A preliminary double-lined spectroscopic orbital solution was reported by Stefanik, Marschall & Nations (1992) with a period of 1.84 days, and also by Baker et al. (1994) who derived a small eccentricity of $e = 0.016$. Our improved solution indicates a circular orbit, and the light ratio between the stars is $l_B/l_A = 0.39 \pm 0.02$. The velocities and orbital elements are given in Table 6 and Table 7, respectively.

Our orbital fit is shown in Figure 2. As in the previous case, the light ratio and mass ratio are consistent with the mass-luminosity relation for dwarfs. If the measurement of the Li I $\lambda 6708$ strength (Table 1) in this double-lined binary is assumed to correspond to the brighter primary, a correction for the dilution produced by the light of the secondary would increase the equivalent width to roughly 0.16 Å. This is much weaker than typical Li strengths for stars of similar temperature in the Pleiades cluster, arguing that TYC 6604-0118-1 is considerably older than the Pleiades (age ~ 120 Myr), and hence is not a member of the TW Hya association. Its center-of-mass velocity is also quite different from that of the member stars. The minimum angle for eclipses to occur is $i_{\min} \approx 77^\circ$, whereas the angle derived assuming normal main-sequence masses for the stars is $i \approx 48^\circ$. The system is detached.

3.3. RXJ1100.0–3813

This object was selected by us as a possible member based on proximity on the sky and the X-ray properties from ROSAT. The observations show it to be a single-lined binary with a period of 1.37 d and a circular orbit. The measured radial velocities are listed in Table 8 and the elements are given in Table 9.

We see no sign of the secondary in our spectra. From an estimated mass for the primary of $1.0 M_\odot$ based on its derived effective temperature, we infer a minimum mass for the secondary of $0.18 M_\odot$ if the orbit is viewed edge-on, corresponding to a spectral type around

M5. If the companion is a main sequence star, it is unlikely to be earlier than about K5 or it would be bright enough that we would have detected its spectral lines. The orbit and our measurements are shown in Figure 3. On the basis of its kinematics this object is unlikely to be a true member of the TW Hya association. No measurements of the Li I $\lambda 6708$ strength are available.

3.4. HD 97131

Also known as HIP 54610, CD–29°8898, and RXJ1110.5–3027, this object is another X-ray source from the ROSAT All Sky Survey that was initially considered a possible member of the TW Hya association. The HIPPARCOS mission later showed that it is much more distant than the other members ($\pi_{\text{HIP}} = 4.86 \pm 1.23$ mas), and in addition the Li I $\lambda 6708$ line is very weak, both of which indicate that it is probably not associated. The systemic velocity is also completely different from that of the known members in the same area of the sky.

The object turned out to be a double-lined triple system. The orbital period of the primary (the brighter star, “A”) is 133.5 d, and the secondary is itself a single-lined binary with a period of 1.76 d. The velocities for the two visible objects (“A” and “Ba”) are given in Table 10. The two orbits were solved simultaneously under the usual approximation that the inner binary acts as a point source located at its center of mass for computing the motion in the outer orbit. Light travel time corrections are relatively small (< 0.001 d) but were applied nevertheless, and are given in Table 10. Table 11 lists the orbital elements of this combined solution. The orbit of the secondary is circular, as expected from its short period, while the wide orbit is slightly eccentric. The fits are shown in Figure 4, which includes a schematic view of the system. The light ratio between the primary and secondary is $l_{\text{Ba}}/l_{\text{A}} = 0.51 \pm 0.02$.

Adopting a typical mass for a main-sequence star with the effective temperature we determine for the primary (which corresponds to SpT \sim F0), the inclination angle of the wide orbit is estimated to be $i_{\text{AB}} \approx 26^\circ$. The total mass of the secondary sub-system implied by this angle is $M \approx 2.3 M_\odot$. Adopting a typical mass for star Ba based on its temperature, and using the mass function of the secondary from our orbital solution, we can also estimate the inclination angle of the orbit of the secondary (i_{B}), which remarkably turns out to be also approximately 26° . The inner and outer orbits may thus be coplanar¹⁰. With these

¹⁰The relative inclination of the two orbits, i_{rel} , depends also on the difference between the position angles of the ascending nodes (Ω) (e.g., Fekel 1981), which can only be determined from astrometry: $\cos i_{\text{rel}} =$

parameters, the measured $v \sin i$ of star Ba and the assumption of spin-orbit synchronization lead to a radius for that star consistent with the expected value for its mass. The unseen star (Bb) is inferred to have a mass $M \approx 0.9 M_{\odot}$ (SpT \sim G7-G8).

3.5. RXJ1115.1–3233

As in the previous case, this star was selected as a candidate member based on its proximity on the sky and its X-ray properties. It is a double-lined binary with a circular orbit and a period of 2.23 d. The secondary is quite faint, with the ratio of the brightness of the two stars being $l_B/l_A = 0.14 \pm 0.02$. The radial-velocity measurements are listed in Table 12, and the orbital elements are given in Table 13. The observations and the orbit are displayed in Figure 5.

Under the assumption that the stars are rotating synchronously with the orbit, the minimum angle for eclipses to occur is $i_{\min} \approx 80^\circ$. However, the minimum masses are large enough (for the temperatures we determine) that the possibility of eclipses cannot be completely ruled out. The system is detached. The mass ratio and light ratio conform to the typical mass-luminosity relation for the main sequence, suggesting the components are probably dwarfs. On the basis of its systemic velocity the system is unlikely to be a true member of the TW Hya association. No measurements of the Li I $\lambda 6708$ strength are available.

4. Stars without orbital solutions

The individual radial velocities for the remaining stars in our sample are collected in Table 14, with the exception of TWA-3A and TWA-5A (see above). The correlation peaks for these two objects display obvious distortions that appear to change considerably on short time scales (a few days), and are presumably the result of blends from the lines of two or more stars of similar brightness. A better understanding of these systems is required before meaningful velocities can be extracted from our spectra.

Several other stars on our target list appear to exhibit variations in their radial velocities that may indicate the presence of companions. Among these, RXJ1109.7–3907 and TWA-12 have one discrepant velocity each. TWA-9A shows a scatter among the 18 velocities

$\cos i_{AB} \cos i_B + \sin i_{AB} \sin i_B \cos(\Omega_{AB} - \Omega_B)$. Nevertheless, the similarity between i_{AB} and i_B is highly suggestive.

available that is about a factor of 2 larger than expected from the internal errors, but no coherent periodicity is seen. Velocity “jitter” at this level could be caused by the presence of spots, which are not uncommon in young objects such as this. The star was also observed by the HIPPARCOS mission (HIP 57589), and the photometric measurements show a dispersion of about 0.07 mag, again roughly twice as large as the mean internal errors and perhaps consistent with the spot hypothesis. No periodicity is detected in the HIPPARCOS photometry.

Our 4 archival spectra for HIP 50796 obtained in 1986 indicate a velocity drift of more than 4 km s^{-1} over an interval of 147 days, which is highly significant compared to the measurement errors. Six observations taken 16 yrs later are some 30 km s^{-1} higher (and show further changes over a 1-month period), confirming that the object is a binary (see Table 14). A recent measurement published by Song, Bessell & Zuckerman (2002) gives an intermediate velocity. Astrometric evidence that the star is a binary is also seen in the HIPPARCOS observations, where acceleration terms (linear changes in the proper motion components) were found to be significant. The period of the system is as yet unknown.

5. Discussion

Table 15 lists the mean radial velocity for each of our targets (10 candidate members, and 10 previously known bona-fide members). For the binaries with solved orbits the value given is the center-of-mass velocity. A comparison with other values from the literature, which are typically less accurate, indicates fairly good agreement.

The previously recognized members of the TW Hya group in our sample (i.e., the ones with TWA- designations in column 2) all have mean radial velocities within about 3 km s^{-1} of each other, supporting their association. In the case of TWA-4 A/B (HD 98800A/B) the 7 km s^{-1} difference between the components is due to orbital motion of the two stars around their center of mass, and is quite large because the pair is currently approaching periastron passage in a fairly eccentric orbit (Torres et al. 1995; Tokovinin 1999). Each of the components is in turn a spectroscopic binary. Since they are of similar mass (Soderblom et al. 1998), it may be assumed that the center of mass of the quadruple system is close to the average of the velocities of the two visual components, or $+9.2 \text{ km s}^{-1}$. Similarly, the average of the velocities of the two components of TWA-13 is $+12.1 \text{ km s}^{-1}$. TWA-2 and TWA-9 are also binaries, but only the velocities of the primaries have been measured.

The lower part of Table 15 collects radial velocity measurements from the literature for other recognized members of the TW Hya association that have them. With the possible

exception of TWA-8A (for which no error estimate is available), the velocities for these stars are again seen to be consistent with those of the other members.

The mean radial velocity of the stars currently believed to belong to the association is thus approximately $+11 \text{ km s}^{-1}$ in the heliocentric frame¹¹. However, due to their proximity ($\sim 60 \text{ pc}$; but see below) they are spread across tens of degrees on the sky, and kinematic studies by Frink (2001) and Makarov & Fabricius (2001) have shown that because of this it is expected that they will exhibit a radial velocity gradient across the region, even if they share a common space velocity. The convergent-point solution by Frink (2001) also showed that the spread in the “kinematic” distance to individual objects within the association (based on the proper motions and an assumed streaming velocity) is very significant, ranging from $\sim 30 \text{ pc}$ to $\sim 120 \text{ pc}$. Good agreement was found between the kinematic distances and the few direct determinations available from the HIPPARCOS mission. However, it was also found that the predicted radial velocities for the known members from this model are too small by several km s^{-1} .

The investigation by Makarov & Fabricius (2001) found a similar spread in distances and radial velocities, but went a step further and incorporated uniform expansion of the association into the kinematic model in order to reproduce the observed radial velocities available at the time. They carried out a search for new members in an area of more than 3000 square degrees by selecting objects with X-ray properties similar to those of known young stars using the ROSAT Bright Source Catalogue (Voges et al. 1999), and kinematic criteria based on proper motions for these X-ray sources from the Tycho-2 catalogue (Høg et al. 2000). In this way they proposed 23 new stars as possible members of the TW Hya association. For each of them they predicted the radial velocity and distance, using their model that includes an expansion term. We have observed four of these candidates, in addition to a number of other bona-fide members also listed by Makarov & Fabricius that satisfy their kinematic criteria. The top section of Table 16 shows these objects, along with their proper motion and their predicted and measured distances (D_{kin} and D_{trig}) and radial velocities (RV_{pred} and RV_{obs}). The bottom section of the table adds 3 other recognized members of the association with velocity measurements from other sources (see Table 15).

The known members typically have measured radial velocities that are quite close to the predicted values. TWA-9A, which we discussed earlier, may be an exception, and we note that its measured distance also differs from the model prediction (by nearly 4σ). The velocity

¹¹The formal average of the velocities of TWA-1, 2, 3, 4, 7, 9, 11, 12, 13, and 19 from Table 15 (with binary components combined into a single value) is $+11.1 \pm 0.4 \text{ km s}^{-1}$; it is $+10.7 \pm 0.5 \text{ km s}^{-1}$ if the somewhat lower value for TWA-8A is included. The uncertainties given correspond to the error of the arithmetic mean.

of TWA-19A shows a rather large deviation from the predicted value as well, although the precision of the observation in this case is not as good.

Of the candidate members proposed by Makarov & Fabricius (2001) that we measured (first 4 entries in Table 16) HIP 48273 and TYC 6604-0118-1 have radial velocities that disagree with the predictions, and HIP 50796 is a binary for which the center-of-mass velocity is not yet known (see §4) but seems unlikely to be as low as the expected value of $+13 \text{ km s}^{-1}$. Song, Bessell & Zuckerman (2002) also reported velocities for these stars, and their values are consistent with our conclusions. HIP 53486 is especially interesting in that it is the nearest candidate member ($\sim 17 \text{ pc}$), and also the one with the lowest predicted radial velocity. The trigonometric parallax as measured by HIPPARCOS agrees very well with the kinematic distance from the model, and our measured radial velocity is only 1.8 km s^{-1} different from the expected value. The velocity measurement of Song, Bessell & Zuckerman (2002) is consistent once again with our own determination. However, the Li I $\lambda 6708$ line as measured by those authors is very weak in all 4 of these objects, which rules them out as young stars and hence as members of the TW Hya association.

In fact, Song, Bessell & Zuckerman (2002) measured most of the other fainter candidate members proposed by Makarov & Fabricius (2001), and found that although some have radial velocities and/or distances similar to the predictions from the kinematic model, the equivalent width of the Li line is very small in all but 3 of them. Those three stars are TYC 7760-0835-1, TYC 8238-1462-1, and TYC 8234-2856-1, which are among the most distant candidate members (D_{pred} ranging from 111 pc to 138 pc). Their measured radial velocities do not agree with the predicted values particularly well, but are based on a single observation and could be affected by orbital motion in a binary. Some evidence for this was presented by Makarov & Fabricius (2001), who reported that a re-reduction of the Tycho-2 observations revealed that both TYC 7760-0835-1 and TYC 8238-1462-1 appear to be close visual binaries with angular separations less than $0''.5$ and magnitude differences (ΔV_T) under 1 mag. Further radial velocity measurements of these candidates are needed to confirm those indications.

With the possible exception of these three stars, it seems that no other new members of the TW Hya association have emerged from the kinematic selection by Makarov & Fabricius (2001). One of the most interesting results of that analysis was their finding that their model required some degree of expansion in the association in order to reproduce the available observations (proper motions, HIPPARCOS distances, and particularly the radial velocities), at a rate of $0.12 \text{ km s}^{-1} \text{ pc}^{-1}$. This implies a dynamical age of 8.3 Myr, remarkably close to other independent estimates that place the age of the association at about 10 Myr. It has been pointed out, however, that the above kinematic study included many candidate

members that are now believed not to be true members of the group (Mamajek & Feigelson 2001), as discussed above. At least 20 such stars out of the 31 objects in the Makarov & Fabricius study contribute to determine the location of the convergent point, the space velocity, the internal velocity dispersion of the association, and the expansion rate. As more radial velocities become available for the bona-fide members, it might prove fruitful to refine the kinematic modeling to see how the inferred properties and the selection of new candidate members change.

Optical and kinematical information for the 20 or so objects currently considered members of the TW Hya association is scattered throughout the literature and is sometimes difficult to track down. For the benefit of the reader we have compiled a list in Table 17 that collects accurate coordinates, spectral types, optical photometry, absolute proper motions, parallaxes (when available from the Hipparcos mission), mean Li I $\lambda 6708$ equivalent widths, and mean heliocentric radial velocities for all objects that have been referred to with a TWA- designation, as well as for a few of the most likely new additions from recent studies mentioned earlier. All currently known visual companions have been included as well, with the exception of those considered to be background objects. A total of at least 11 of the 19 objects are in visual binary systems or in systems of higher multiplicity (triples and quadruples) that include also spectroscopic companions. This represents a fairly high fraction that seems consistent with the large binary frequency found for young stars in other populations (see, e.g., Mathieu 1994). We point out, however, that demonstrating that all these stars with TWA- designations are truly associated with each other is by no means trivial. In fact, suggestions that some of them may actually belong instead to other nearby groups have already been made (e.g., Mamajek & Feigelson 2001; Song, Bessell & Zuckerman 2002), so it is entirely possible that future kinematic studies may reduce the list of true members.

Referring back to Table 1, it is rather striking that of the 10 candidate members that we have examined in this paper (none of which turned out to be a true member of the TW Hya association), no less than 6 are confirmed binaries. Four are double-lined and the other two single-lined. Furthermore, of the binaries with orbital solutions, *all of them* have periods of 3 days or less. This is most likely due to a selection effect. All these stars were chosen in part based on their X-ray emission (detection by ROSAT), with the idea that this would preferentially pick out young objects. Instead it seems to have favored the inclusion of active objects in the form of close binaries that are synchronized. The X-ray emission observed in these cases is therefore not a sign of youth but rather of rapid rotation maintained by tidal coupling in short-period binaries. We note that the outer orbit of the triple system HD 97131 is actually quite long (133.5 d), but it is the secondary (which is itself a binary) that is probably responsible for the X-ray emission, since its orbital period is only 1.76 d.

This highlights the danger of relying heavily on X-ray emission when trying to identify young stars. Many of them will prove to be older synchronized binaries. A similar conclusion was reached recently in a much larger sample of ROSAT-selected sources by Torres, Neuhäuser & Guenther (2002).

6. Conclusions

The study of loose associations of young nearby stars has received considerable attention in the past few years and is beginning to provide valuable new glimpses into the history of star formation in the vicinity of the Sun (see, e.g., Jayawardhana & Greene 2001). In this paper we report spectroscopic results for members and candidate members of the TW Hya association based on multiple observations per object, which have revealed several binary and multiple systems that had gone unnoticed in many previous studies based on a single radial-velocity measurement. Orbital elements have been derived for 5 of these systems, including the systemic velocities.

None of the 10 potential new members on our list turn out to be true members of the association, based on our radial velocity results and measurements of the Li I $\lambda 6708$ line strength and other velocity measurements reported by Song, Bessell & Zuckerman (2002). The fact that many of them are binaries with short orbital periods is understood as a selection effect stemming from the use of X-ray emission as one of the criteria to favor the inclusion of young objects. Although X-ray emission may indeed be a common characteristic of pre-main sequence stars, it is shared by a variety of other older active systems as well.

A number of objects that do belong to the group and that are known or suspected to be spectroscopic binaries such as TWA-3A, TWA-5A, TWA-12, and others, still require radial velocity monitoring to determine their dynamical properties. The determination of the line-of-sight motion for these objects and for other potential members that may be identified in the future is an important complement to the proper-motion studies of groups such as the TW Hya association, and to our understanding of their relation to larger groups of young stars within a few hundred parsecs of the Sun.

Many of the spectroscopic observations for this project were obtained by P. Berlind, J. Caruso, M. Calkins, R. J. Davis, and J. Zajac. and we thank R. J. Davis for also maintaining the CfA echelle database. Helmut Abt, the referee, provided a number of comments and suggestions that were very helpful. RN wishes to acknowledge financial support from the Bundesministerium für Bildung und Forschung through the Deutsche Zentrum für Luft- und Raumfahrt e.V. (DLR) under grant number 50 OR 0003. This research has made use of

the SIMBAD database, operated at CDS, Strasbourg, France, and of NASA's Astrophysics Data System Abstract Service.

REFERENCES

- Alencar, S. H. P., & Batalha, C. 2002, *ApJ*, 571, 378
- Baker, A. J., Stefanik, R. P., Marschall, L. A., Latham, D. W., & Nations, H. L. 1994, in Eighth Cambridge Workshop on Cool Stars, Stellar Systems and the Sun, ASP Conf. Ser. 64, ed. J.-P. Caillaut (San Francisco: ASP), 551
- Barbier-Brossat, M., & Figon, P. 2000, *A&AS*, 142, 217
- Bodenheimer, P. 1965, *ApJ*, 142, 451
- Cruddace R. G., Hasinger G. R., Schmitt J. H. M. M. 1988, in *Astronomy From Large Databases*, ESO Conference and Workshop Proc. 28, eds. F. Murtagh & A. Heck (Garching), p. 177
- de Jager, C., & Nieuwenhuijzen, H. 1987, *A&A*, 177, 217
- de la Reza, R., Torres, C. A. O., Quast, G., Castillo, B. V., & Vieira, G. L. 1989, *ApJ*, 343, L61
- Favata, F., Barbera, M., Micela, G., & Sciortino, S. 1995, *A&A*, 295, 147
- Fekel, F. C. 1981, *ApJ*, 246, 879
- Fleming, T. A. 1988, Ph.D. Thesis, Univ. of Arizona
- Flower, P. J. 1996, *ApJ*, 469, 355
- Frink, S. 2001, in *Young Stars Near Earth: Progress and Prospects*, ASP Conf. Ser. 244, eds. R. Jayawardhana & T. P. Greene, (San Francisco: ASP), 16
- Gioia, I. M., Maccacaro, T., Schild, R. E., Wolter, A., Stocke, J. T., Morris, S. L., & Henry, J. P. 1990, *ApJS*, 72, 567
- Gizis, J. E. 2002, *ApJ*, 575, 484
- Gray, D. F. 1992, *The Observation and Analysis of Stellar Photospheres*, 2nd Ed. (Cambridge: Cambridge Univ. Press), 431

- Gregorio-Hetem, J., Lépine, J. R. D., Quast, G., Torres, C. A. O., & de la Reza, R. 1992, *AJ*, 103, 549
- Guenther, E., Neuhäuser, R., Huélamo, N., Brandner, W., & Alves, J. 2001, *A&A*, 365, 514
- Hearty, T., Fernández, M., Alcalá, J. M., Covino, E., Neuhäuser, R. 2000, *A&A*, 357, 681
- Hearty, T., Neuhäuser, R., Stelzer, B., Fernández, M., Alcalá, J. M., Covino, E., & Hambaryan, V. 2000, *A&A*, 353, 1044
- Henize, K. G. 1976, *ApJS*, 30, 491
- Herbig, G. H. 1978, in *Problems of Physics and Evolution of the Universe*, ed. L. V. Mirzoyan (Yeravan: Armenian Academy of Sci.), 171
- Hoff, W., Alcalá, J. M., & Sterzik, M. F. 1997, in *Cool Stars in Clusters and Associations: Magnetic Activity and Age Indicators*, eds. G. Micela, R. Pallavicini & S. Sciortino, *Mem. Soc. Astr. It.* (abstract booklet), 68(4), 31
- Hoff, W., Henning, T., & Pfau, W. 1998, *A&A*, 336, 242
- Høg, E., Fabricius, C., Makarov, V. V., Urban, S., Corbin, T., Wycoff, G., Bastian, U., Schwekendiek, P., & Wicenec, A. 2000, *A&A*, 355, L27
- Jayawardhana, R., & Greene, T. P. (eds.) 2001, *Young Stars Near Earth: Progress and Prospects*, *ASP Conf. Ser.* 244, (San Francisco: ASP)
- Kastner, J. H., Zuckerman, B., Weintraub, D. A., & Forveille, T. 1997, *Science*, 277, 67
- Kurtz, M. J., & Mink, D. J. 1998, *PASP*, 110, 934
- Latham, D. W. 1992, in *IAU Coll. 135, Complementary Approaches to Double and Multiple Star Research*, eds. H. A. McAlister & W. I. Hartkopf (San Francisco: ASP), 110
- Latham, D. W., Nordström, B., Andersen, J., Torres, G., Stefanik, R. P., Thaller, M., & Bester, M. 1996, *A&A*, 314, 864
- Latham, D. W., Stefanik, R. P., Torres, G., Davis, R. J., Mazeh, T., Carney, B. W., Laird, J. B., & Morse, J. A. 2002, *AJ*, 124, 1144
- Leggett, S. K., Allard, F., Berriman, G., Dahn, C. C., & Hauschildt, P. H. 1996, *ApJS*, 104, 117
- Lowrance, P. J., McCarthy, C., & Becklin, E. E. 1999, *ApJ*, 512, L69

- Macintosh, B., Max, C., Zuckerman, B., Becklin, E. E., Kaisler, D., Lowrance, P., Weinberger, A., Christou, J., Schneider, G., & Acton, S. 2001, in *Young Stars Near Earth: Progress and Prospects*, ASP Conf. Ser. 244, eds. R. Jayawardhana & T. P. Greene, (San Francisco: ASP), 309
- Makarov, V. V., & Fabricius, C. 2001, *A&A*, 368, 866
- Mamajek, E. E., & Feigelson, E. D. 2001, in *Young Stars Near Earth: Progress and Prospects*, ASP Conf. Ser. 244, eds. R. Jayawardhana & T. P. Greene, (San Francisco: ASP), 104
- Mamajek, E. E., Lawson, W. A., & Feigelson, E. D. 1999, *ApJ*, 516, L77
- Mamajek, E. E., Lawson, W. A., & Feigelson, E. D. 2000, *ApJ*, 544, 356
- Mathieu, R. D. 1994, *ARA&A*, 32, 465
- Mayor, M., & Mazeh, T. 1987, *A&A*, 171, 157
- Muzerolle, J., Calvet, N., Briceño, C., Hartmann, L., & Hillenbrand, L. 2000, *ApJ*, 535, L47
- Neuhäuser, R., Brandner, W., Eckart, A., Guenther, E., Alves, J., Ott, T., Huélamo, N., & Fernández, M. 2000b, *A&A*, 354, L9
- Neuhäuser, R., Guenther, E. W., Petr, M. G., Brandner, W., Huélamo, N., & Alves, J. 2000a, *A&A*, 360, L39
- Neuhäuser, R., Sterzik, M. F., Schmitt, J. H. M. M., Wichmann, R., & Krautter, J. 1995, *A&A*, 297, 391
- Neuhäuser, R., Torres, G., Sterzik, M. F., & Randich, S. 1997, *A&A*, 325, 647
- Nordström, B., Latham, D. W., Morse, J. A., Milone, A. A. E., Kurucz, R. L., Andersen, J., & Stefanik, R. P. 1994, *A&A*, 287, 338
- Popper, D. M. 1949, *ApJ*, 109, 100
- Popper, D. M. 1980, in *IAU Symp. 88, Close Binary Stars: Observations and Interpretations*, eds. M. J. Plavec, D. M. Popper & R. K. Ulrich (Dordrecht: Reidel), 387
- Popper, D. M., & Shajn, G. A. 1948, *Publ. Crimean Ap. Obs.*, 2, 44
- Reipurth, B., Pedrosa, A., & Lago, M. T. V. T. 1996, *A&AS*, 120, 229
- Rucinski, S. M., & Krautter, J. 1983, *A&A*, 121, 217

- Shajn, G. A. 1932, *Plukovo Obs. Circ.*, 2, 11
- Skumanich, A. 1972, *ApJ*, 171, 565
- Soderblom, D. R., Henry, T. J., Shetrone, M. D., Jones, B. F., & Saar, S. H. 1996, *ApJ*, 460, 984
- Soderblom, D. R., King, J. R., Siess, L., Noll, K. S., Gilmore, D. M., Henry, T. J., Nelan, E., Burrows, C. J., Brown, R. A., Perryman, M. A. C., Benedict, G. F., McArthur, B. J., Franz, O. G., Wasserman, L. H., Jones, B. F., Latham, D. W., Torres, G., & Stefanik, R. P. 1998, *ApJ*, 498, 385
- Song, I., Bessell, M. S., & Zuckerman, B. 2002, *A&A*, 385, 862
- Stauffer, J. R., Hartmann, L. W., & Barrado y Navascués, D. 1995, *ApJ*, 454, 910
- Stefanik, R. P., Latham, D. W., & Torres, G. 1999, in *IAU Coll. 170, Precise Stellar Radial Velocities*, eds. J. B. Hearnshaw & C. D. Scarfe (San Francisco: ASP), 354
- Stefanik, R. P., Marschall, L. A., & Nations, H. L. 1992, in *IAU Coll. 135, Complementary Approaches to Double and Multiple Star Research*, eds. H. A. McAlister & W. I. Hartkopf (San Francisco: ASP), 389
- Sterzik, M. F., Alcalá, J. M., Covino, E., & Petr, M. G. 1999, *A&A*, 346, L41
- Stoche, J. T., Morris, S. L., Gioia, I. M., Maccacaro, T., Schild, R. E., Wolter, A., Fleming, T. A., & Henry, J. P. 1991, *ApJS*, 76, 813
- Tokovinin, A. A. 1999, *Astron. Lett.*, 25, 669
- Torres, G., Neuhäuser, R., & Guenther, E. W. 2002, *AJ*, 123, 1701
- Torres, G., Neuhäuser, R., & Latham, D. W. 2001, in *Young Stars Near Earth: Progress and Prospects*, ASP Conf. Ser. 244, eds. R. Jayawardhana & T. P. Greene, (San Francisco: ASP), 283
- Torres, G., Stefanik, R. P., Latham, D. W., & Mazeh, T. 1995, *ApJ*, 452, 870
- Torres, C. A. O., da Silva, L., Quast, G., de la Reza, R., & Jilinski, E. 2000, *AJ*, 120, 1410
- van den Ancker, M. E., Pérez, M. R., & de Winter, D. 2001, *Young Stars Near Earth: Progress and Prospects*, ASP Conf. Ser. 244, eds. R. Jayawardhana & T. P. Greene (San Francisco: ASP), 69

- Voges, W., Aschenbach, B., Boller, Th., Bräuninger, H., Briel, U., Burkert, W., Dennerl, K., Englhauser, J., Gruber, R., Haberl, F., Hartner, G., Hasinger, G., Kürster, M., Pfeffermann, E., Pietsch, W., Predehl, P., Rosso, C., Schmitt, J. H. M. M., Trümper, J., & Zimmermann, H. U. 1999, *A&A*, 349, 389
- Webb, R. A., Zuckerman, B., Platais, I., Patience, J., White, R. J., Schwartz, M. J., & McCarthy, C. 1999, *ApJ*, 512, L63
- Zacharias, N., Urban, S. E., Zacharias, M. I., Hall, D. M., Wycoff, G. L., Rafferty, T. J., Germain, M. E., Holdenried, E. R., Pohlman, J. W., Gauss, F. S., Monet, D. G., & Winter, L. 2000, *AJ*, 120, 2131
- Zucker, S., & Mazeh, T. 1994, *ApJ*, 420, 806
- Zuckerman, B. 2001, *Young Stars Near Earth: Progress and Prospects*, ASP Conf. Ser. 244, R. Jayawardhana & T. P. Greene (San Francisco: ASP), 122
- Zuckerman, B., Song, I., Bessell, M. S., & Webb, R. A. 2001a, *ApJ*, 562, L87
- Zuckerman, B., & Webb, R. A. 2000, *ApJ*, 535, 959
- Zuckerman, B., Webb, R. A., Schwartz, M., & Becklin, E. E. 2001b, *ApJ*, 549, L233

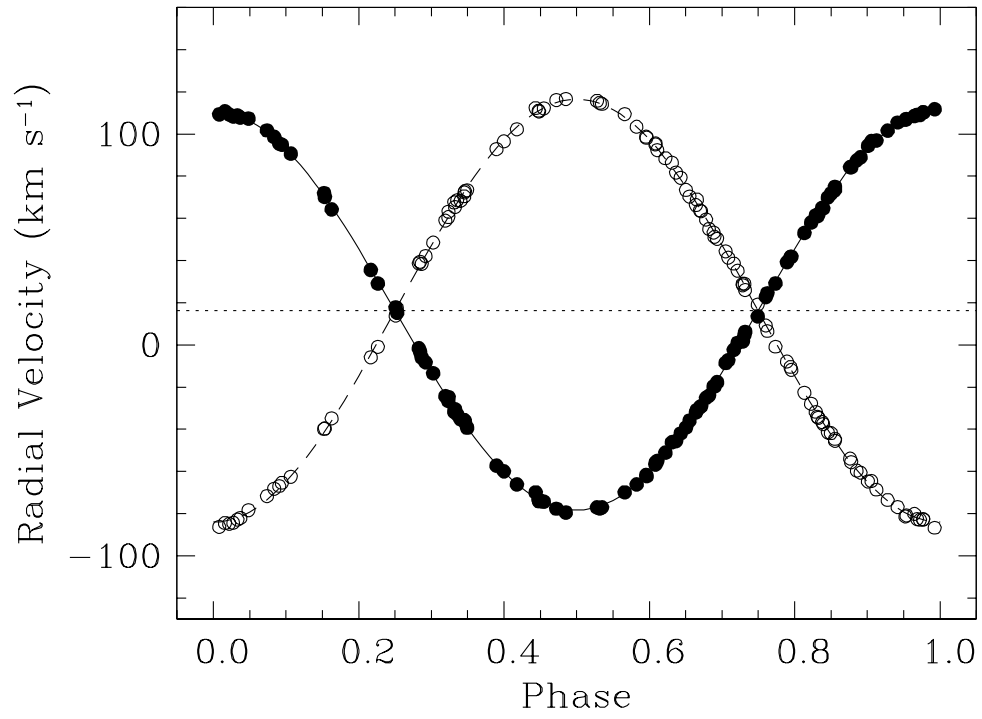


Fig. 1.— Radial velocity observations for HIP 48273 (filled circles for the primary) along with our orbital solution. The center-of-mass velocity is indicated by the dotted line.

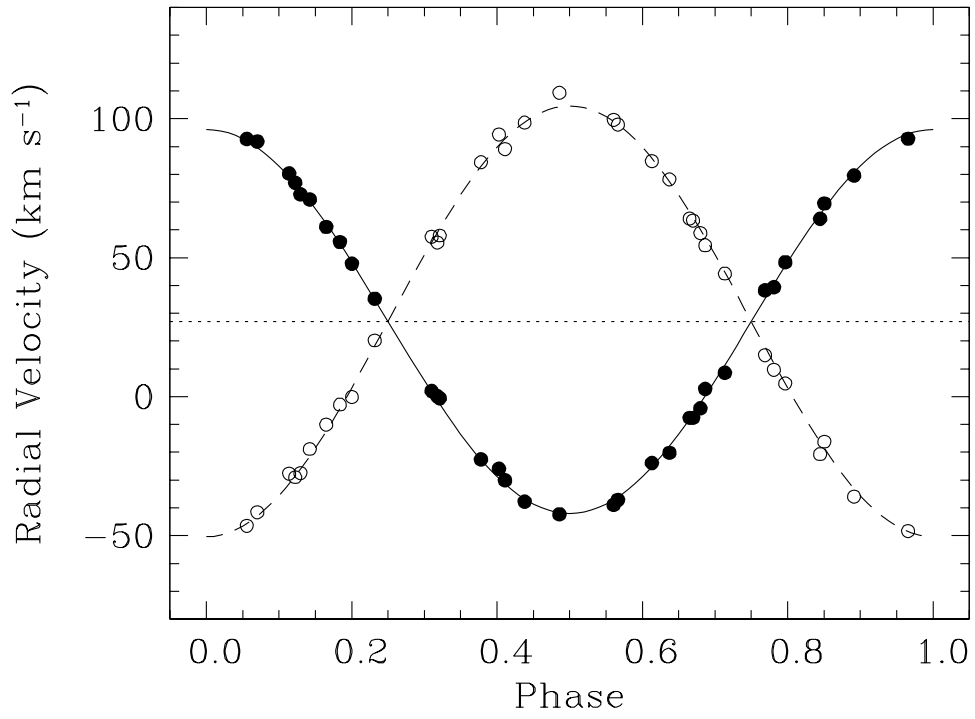


Fig. 2.— Radial velocity observations for TYC 6604-0118-1 (filled circles for the primary) along with our orbital solution. The center-of-mass velocity is indicated by the dotted line.

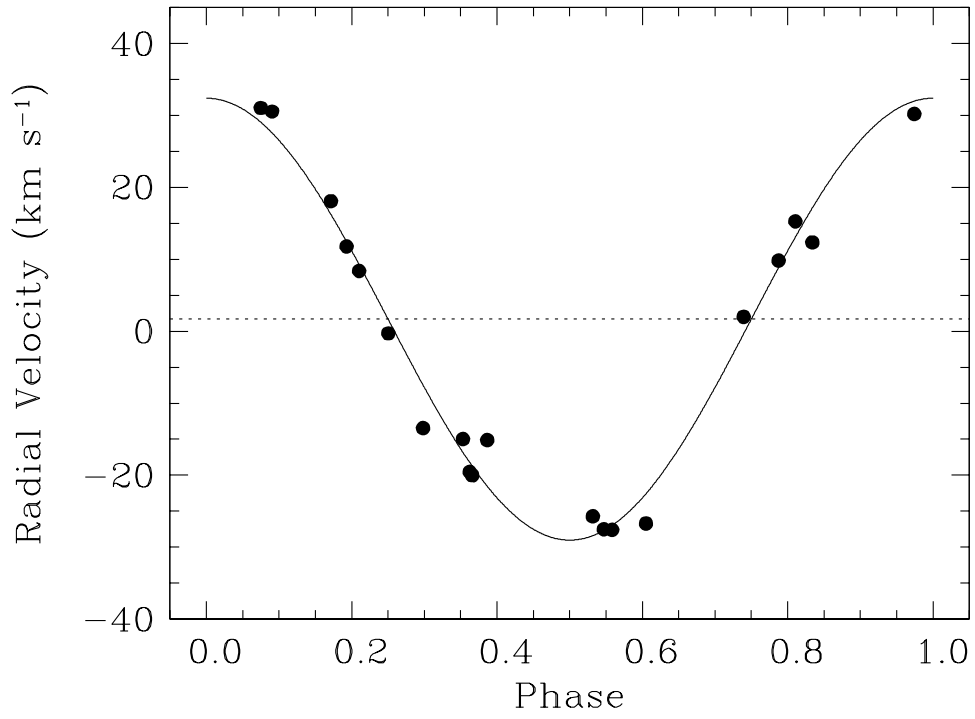


Fig. 3.— Radial velocity observations for RXJ1100.0–3813 along with our orbital solution. The center-of-mass velocity is indicated by the dotted line.

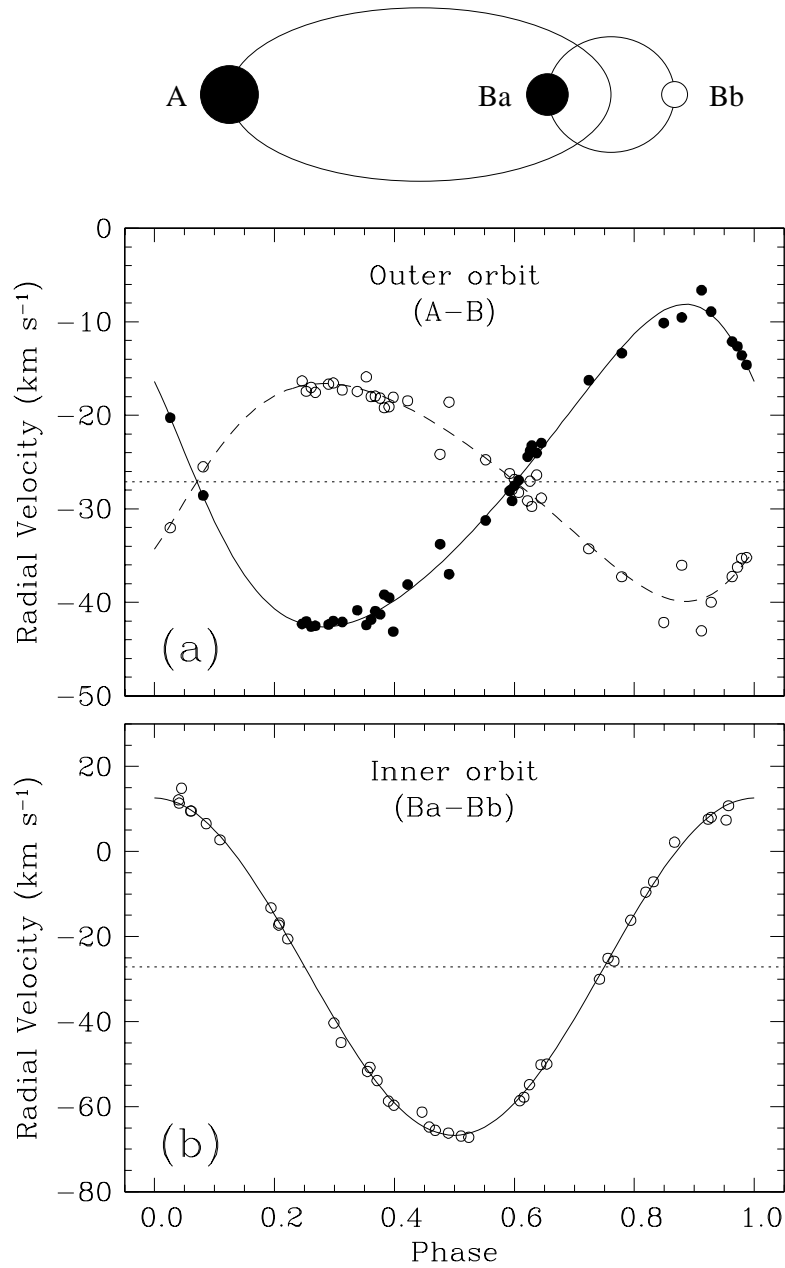


Fig. 4.— Schematic view of the HD 97131 triple system, and radial-velocity observations along with our orbital solutions for the inner and outer orbits. The systemic velocity is indicated by the dotted lines. (a) Outer orbit with a period of 133 d. The primary (A) is indicated by the filled circles, and the motion of the secondary (Ba, open circles) in the inner orbit has been removed; (b) Inner orbit for the secondary, with the velocity of the visible star corrected for motion in the wide orbit.

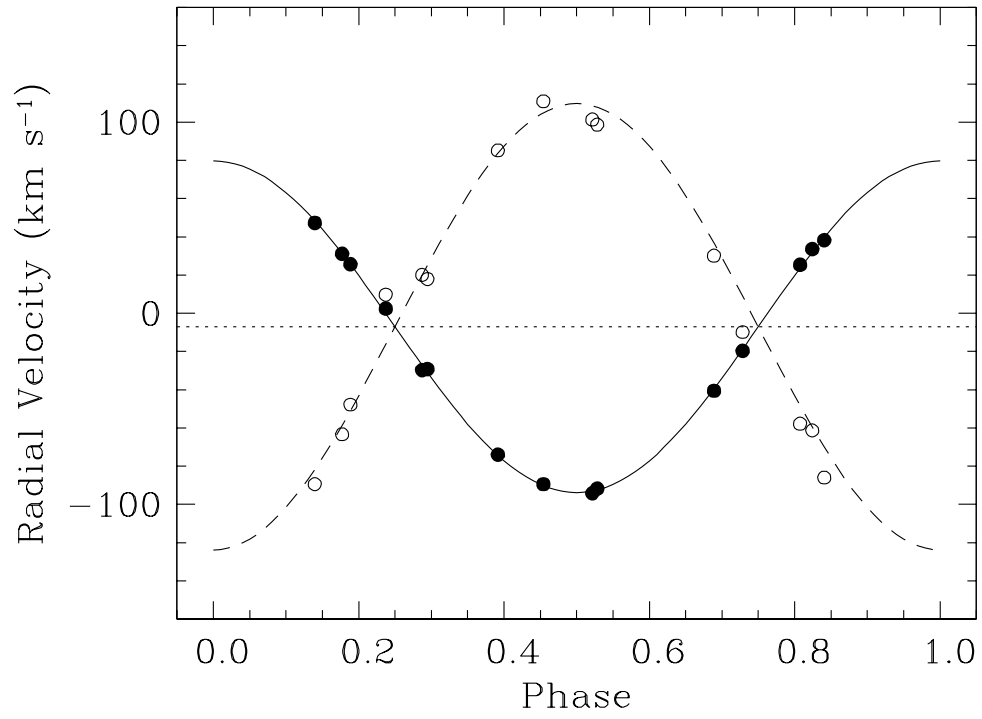


Fig. 5.— Radial velocity observations for RXJ1115.1–3233 (filled circles for the primary) along with our orbital solution. The center-of-mass velocity is indicated by the dotted line.

Table 1. Summary of optical properties.

TWA #	Other name	R.A. (J2000)	Dec. (J2000)	V (mag)	SpT	Li I λ 6708 eq. width (\AA) ^a
1	HIP 48273	09:50:30.1	+04:20:37	6.24	F6	0.021+0.023
2	TYC 6604-0118-1	09:59:08.4	-22:39:35	10.09	K2	0.118
3	HIP 50796	10:22:18.0	-10:32:15	10.80	...	< 0.010
4	HIP 53486	10:56:31.0	+07:23:19	7.37	K0	< 0.010
5	RXJ1100.0-3813	11:00:02.4	-38:13:20	12.29
6	HD 95490	11:00:51.2	-35:33:38	8.79	F7-8	0.13
7	TWA-1 TW Hya	11:01:52.0	-34:42:16	10.92 ^b	K7e	0.426
8	TWA-2A CD-29°8887A	11:09:13.9	-30:01:39	11.07	M2e	0.494
9	RXJ1109.7-3907	11:09:40.1	-39:06:48	10.58	G3	0.190
10	TWA-3A Hen 3-600A	11:10:28.0	-37:31:53	12.04	M3e	0.563
11	HD 97131	11:10:34.2	-30:27:19	9.01	F2	0.03
12	CD-37°7097	11:12:42.7	-38:31:04	10.24	F5	0.11
13	RXJ1115.1-3233	11:15:06.9	-32:32:46	12.36
14	TWA-12 RXJ1121.1-3845	11:21:05.5	-38:45:17	12.85	M2	0.530
15	TWA-13A RXJ1121.3-3447N	11:21:17.3	-34:46:47	11.46	M2e	0.650
16	TWA-13B RXJ1121.3-3447S	11:21:17.5	-34:46:51	12.00	M1e	0.570
17	TWA-4A HD 98800A	11:22:05.3	-24:46:40	9.41 ^b	K4-5	0.425
18	TWA-4B HD 98800B	11:22:05.3	-24:46:39	9.94 ^b	K7+M1	0.335+0.450
19	TWA-5A CD-33°7795A	11:31:55.4	-34:36:27	11.54	M1.5	0.572
20	TWA-9A CD-36°7429A	11:48:24.3	-37:28:49	11.26	K5	0.47

^aAverage of measurements taken from de la Reza et al. (1989), Favata et al. (1995), Soderblom et al. (1996), Kastner et al. (1997), Hoff, Henning & Pfau (1998), Sterzik et al. (1999), Webb et al. (1999), Hoff (1999), Torres et al. (2000), Zuckerman et al. (2001), Song, Bessell & Zuckerman (2002), and new measurements obtained here (see §2). In the case of the binaries these values are not corrected for the presence of the companion.

^bVariable.

Table 2. Summary of X-ray properties based on ROSAT observations.

TWA #	Other name	R.A. ^a (J2000)	Dec. ^a (J2000)	σ^b ($''$)	ML^c	Exposure (s)	Count rate (s^{-1})	Hardness ratios ^d HR1 HR2	
1	HIP 48273	09:50:30.2	+04:20:47	8	166	417	0.181 ± 0.022	-0.15 ± 0.12	$+0.07 \pm 0.18$
2	TYC 6604-0118-1	09:59:08.2	-22:39:34	8	230	512	0.418 ± 0.044	-0.15 ± 0.10	-0.12 ± 0.15
3	HIP 50796	10:22:19.2	-10:33:02	31	18	404	0.068 ± 0.016	$+0.06 \pm 0.26$	-0.05 ± 0.38
4	HIP 53486	10:56:30.6	+07:23:14	11	183	344	0.153 ± 0.022	-0.36 ± 0.14	-0.44 ± 0.26
5	RXJ1100.0-3813	11:00:05.2	-38:13:12	32	9	244	0.036 ± 0.015	$+0.42 \pm 0.45$	-0.54 ± 0.73
6	HD 95490	11:00:52.8	-35:33:14	24	11	375	0.045 ± 0.015	-0.56 ± 0.25	$+0.04 \pm 0.67$
7	TWA-1 TW Hya	11:01:52.0	-34:42:12	7	588	337	0.571 ± 0.044	$+0.58 \pm 0.06$	-0.12 ± 0.08
8	TWA-2 CD-29°8887	11:09:13.5	-30:01:33	8	228	325	0.341 ± 0.035	-0.22 ± 0.09	-0.02 ± 0.15
9	RXJ1109.7-3907	11:09:40.0	-39:06:57	11	76	367	0.116 ± 0.020	$+0.15 \pm 0.16$	$+0.08 \pm 0.21$
10	TWA-3 Hen 3-600	11:10:28.9	-37:32:04	10	173	336	0.278 ± 0.032	-0.01 ± 0.11	-0.06 ± 0.16
11	HD 97131	11:10:32.8	-30:27:38	38	9	239	0.030 ± 0.013	$+1.00 \pm 0.24$	-0.02 ± 0.15
12	CD-37°7097	11:12:41.9	-38:31:21	15	10	377	0.023 ± 0.009	-0.04 ± 0.39	-1.00 ± 1.75
13	RXJ1115.1-3233	11:15:06.7	-32:33:00	23	14	281	0.046 ± 0.015	$+1.00 \pm 0.39$	-0.25 ± 0.30
14	TWA-12 RXJ1121.1-3845	11:21:05.2	-38:45:29	17	18	94	0.117 ± 0.041	-0.03 ± 0.37	-0.17 ± 1.27
15/16	TWA-13 RXJ1121.3-3447	11:21:17.1	-34:46:44	8	446	473	0.429 ± 0.032	-0.08 ± 0.07	$+0.03 \pm 0.11$
17/18	TWA-4 HD 98800	11:22:05.4	-24:46:32	7	529	330	0.656 ± 0.046	$+0.06 \pm 0.06$	-0.02 ± 0.10
19	TWA-5 CD-33°7795	11:31:55.7	-34:36:32	8	234	122	0.656 ± 0.076	-0.31 ± 0.10	$+0.29 \pm 0.18$
20	TWA-9 CD-36°7429	11:48:24.0	-37:28:38	9	106	122	0.344 ± 0.056	-0.23 ± 0.16	-0.18 ± 0.26

^aX-ray position from ROSAT.

^bUncertainty in the X-ray position.

^cMaximum Likelihood estimator (see text).

^dX-ray hardness ratios are constructed from the integrated counts in three different ROSAT PSPC energy bands: 0.1–0.4 keV (soft), 0.5–0.9 keV (hard 1), and 0.9–2.0 keV (hard 2). For the definition of the hardness ratios in terms of the count levels in these three energy bands, see Neuhäuser et al. (1995).

Table 3. Effective temperatures and projected rotational velocities for the stars in our sample.

TWA #	Other names	SpT	T_{eff} from CfA ^a (K)	T_{eff} from SpT ^b (K)	Other T_{eff} ^c (K)	$v \sin i$ from CfA (km s^{-1})	Other $v \sin i$ ^c (km s^{-1})
1	HIP 48273	F6	6300+6150	6530		22+22	9+14
2	TYC 6604-0118-1	K2	5050+4850	4840		19+15	15, 19, 20
3	HIP 50796	...	4700	...		2	8
4	HIP 53486	K0	5050	5150		1:	1
5	RXJ1100.0-3813	...	5800	...		34	
6	HD 95490	F7-8	6450	6320		13	
7	TWA-1 TW Hya	K7e	4150	4150	4000, 4150	4	4, 5, 10, 13, 14, 15
8	TWA-2A CD-29°8887A	M2e	3670:	3520	3600	13:	13, 15
9	RXJ1109.7-3907	G3	6100	5710	5800	26	23
10	TWA-3A Hen 3-600A	M4e		3290	3400	20:	15
11	HD 97131	F2	7000+6650	7050		19+17	
12	CD-37°7097	F5	6250	6650		14	
13	RXJ1115.1-3233	...	5700+5000:	...		25+10:	
14	TWA-12 RXJ1121.1-3845	M2	3670:	3520	3600	15:	21
15	TWA-13A RXJ1121.3-3447N	M2e	4500	3520	3600	10	10, 16
16	TWA-13B RXJ1121.3-3447S	M1e	4500	3660	3700, 3800	10	12, 16
17	TWA-4A HD 98800A	K4-5		4470	4350		5
18	TWA-4B HD 98800B	K7+M1		4150+3660	4250+3700		3+2
19	TWA-5A CD-33°7795A	M1.5		3590	3500, 3700	36:	58
20	TWA-9A CD-36°7429A	K5	4650	4410		10	

^aValues for the coolest objects are based on the spectral type of the star used as the template, along with the calibration by de Jager & Nieuwenhuijzen (1987).

^bThe calibration adopted is that of de Jager & Nieuwenhuijzen (1987).

^cDeterminations by Fleming (1988), Soderblom et al. (1996), Leggett et al. (1996), Soderblom et al. (1998), Sterzik et al. (1999), Torres et al. (2000), Muzerolle et al. (2000), Song et al. (2002), and Alencar & Batalha (2002).

Table 4. Radial velocity measurements of HIP 48273
(converted to the heliocentric frame) and residuals from the
orbital solution.

HJD (2,400,000+)	RV _A (km s ⁻¹)	RV _B (km s ⁻¹)	(O-C) _A (km s ⁻¹)	(O-C) _B (km s ⁻¹)	Orbital Phase ^a
45817.6815	-31.19	+68.12	-0.82	+2.35	0.332
45817.6942	-33.15	+69.30	-0.65	+1.28	0.336
46438.7980	-29.50	+64.58	-0.50	+0.26	0.670
46459.7471	-76.48	+115.50	+0.22	+0.71	0.529
46485.7095	+109.15	-83.38	-0.29	-1.21	0.028
46744.9328	+89.23	-60.77	-0.50	+0.54	0.891
46771.8911	-2.91	+36.72	+0.30	-0.31	0.717
46803.8013	+64.73	-34.95	-0.53	+0.47	0.163
46812.7237	+98.55	-68.94	+0.64	+1.03	0.084
46816.7986	-66.03	+102.68	+0.05	-0.88	0.418
46832.7825	-39.40	+73.61	-0.73	-0.94	0.651
46833.7536	+108.91	-81.79	-0.22	+0.06	0.969
46838.7627	-56.71	+95.20	+0.20	+1.34	0.609
46863.6641	+22.89	+7.80	-0.02	-1.59	0.761
46926.5454	-36.22	+73.49	+1.50	-0.06	0.347
47104.9434	+19.43	+11.75	+3.12	-4.62	0.750
47114.8976	+109.66	-85.10	-1.11	-1.52	0.009
47114.9215	+110.91	-83.43	+0.51	-0.24	0.017
47141.8532	+62.90	-34.60	-0.71	-0.92	0.833
47163.8478	+109.04	-81.47	+0.25	+0.01	0.034
47167.8167	-30.45	+66.04	+0.38	-0.21	0.333
47172.7651	+106.78	-80.28	-0.05	-0.87	0.953
47198.7018	-69.86	+111.82	+2.60	+1.51	0.444
47202.8131	+39.73	-7.60	-0.17	+0.99	0.790
47214.7235	-19.64	+53.93	-0.75	+0.31	0.689
47216.7297	-35.92	+73.03	+1.39	-0.09	0.346
47218.6590	+110.37	-81.71	+0.39	+1.03	0.978
47220.7575	-31.81	+67.06	+0.18	-0.43	0.665
47221.6058	+105.47	-76.51	+0.70	+0.72	0.942
47222.8380	-35.74	+70.90	+1.43	-2.06	0.346
47226.7667	-45.81	+86.18	+1.76	+2.21	0.632
47228.6592	+13.64	+19.61	-1.84	+2.36	0.251
47229.7529	-55.85	+95.38	+0.87	+1.73	0.609
47309.5385	+2.66	+27.43	-1.43	-1.87	0.729
47320.5701	-35.08	+68.91	-0.35	-1.47	0.341
47481.8904	+72.29	-39.88	+1.85	+1.02	0.153
47491.8099	-59.70	+96.76	+0.63	-0.71	0.400
47495.8759	+5.31	+28.42	-0.11	+0.53	0.732
47510.9493	-30.98	+69.68	+0.18	+3.07	0.666
47511.7503	+101.32	-73.99	-0.20	-0.20	0.928
47517.8127	+96.65	-69.28	-0.52	-0.09	0.913
47526.8939	+87.43	-59.74	-0.28	-0.56	0.886
47538.8374	+42.43	-12.04	-0.93	+0.21	0.796
47544.7519	+6.90	+26.27	+1.01	-1.13	0.732
47550.8293	+0.61	+33.14	+0.84	-0.73	0.722
47570.6993	+28.96	+0.33	-1.05	-1.55	0.227
47583.7081	-79.20	+116.41	-1.36	+0.41	0.486
47599.5499	-28.70	+64.08	-0.47	+0.58	0.672

Table 4—Continued

HJD (2,400,000+)	RV_A (km s^{-1})	RV_B (km s^{-1})	$(O-C)_A$ (km s^{-1})	$(O-C)_B$ (km s^{-1})	Orbital Phase ^a
47608.5636	-50.95	+88.00	+0.51	-0.09	0.623
47627.6037	+73.75	-44.60	-1.03	+0.89	0.856
47642.5930	+23.94	+6.06	-0.20	-2.03	0.763
47666.5670	-55.50	+92.01	+0.40	-0.78	0.612
47701.6324	+95.34	-67.39	-0.47	+0.36	0.091
47813.9046	+69.97	-41.95	-0.17	-1.36	0.846
47837.8417	-24.20	+55.30	-1.75	-2.09	0.683
47848.9001	-14.17	+48.91	+0.39	-0.13	0.303
47865.8629	+75.33	-45.69	+0.47	-0.11	0.856
47879.9641	-77.15	+115.82	-0.33	+0.89	0.473
47899.8206	+109.15	-81.99	-0.41	+0.31	0.973
47908.7657	+94.22	-65.08	+0.85	+0.09	0.901
47930.6760	+101.49	-72.14	+0.72	+0.85	0.074
47940.6810	-38.70	+73.68	+0.44	-1.37	0.350
47952.7253	-8.45	+42.29	+0.33	-0.63	0.293
47969.6652	+65.82	-36.72	-0.43	-0.25	0.838
47987.5871	-9.14	+44.65	+0.51	+0.80	0.706
48000.5988	+108.59	-79.20	-0.09	+2.17	0.965
48014.5493	-77.63	+113.74	-1.36	-0.60	0.532
48026.5324	-73.99	+111.81	+0.55	-0.70	0.455
48191.9106	-61.14	+99.03	+0.35	+0.33	0.596
48204.9057	+71.93	-41.87	-0.20	+0.82	0.850
48221.8274	-57.03	+92.78	-0.45	-0.73	0.390
48232.9692	+108.11	-81.05	-0.16	-0.12	0.038
48251.8451	+35.86	-4.75	+0.18	-0.62	0.217
48266.7819	+91.42	-62.88	+1.15	-0.99	0.107
48281.7066	+111.43	-86.16	+0.61	-2.53	0.993
48283.8002	-25.24	+60.16	-0.53	+0.37	0.679
48308.6504	+53.42	-22.90	+0.14	-0.16	0.814
49702.9923	-6.30	+37.63	-0.89	-1.73	0.287
49755.8241	-65.89	+103.64	-0.17	+0.46	0.583
49787.7123	+109.64	-83.94	-0.35	-1.18	0.022
49819.5606	-73.80	+110.30	-0.48	-0.92	0.449
49847.6283	-45.24	+81.18	-0.03	-0.30	0.637
50030.9234	-42.08	+79.30	+0.25	+0.87	0.643
50058.9630	+58.83	-27.90	+0.65	+0.03	0.823
50098.8414	+84.32	-55.21	-0.20	+0.59	0.878
50114.7755	+94.89	-65.94	+0.19	+0.63	0.095
50139.7933	-3.83	+38.24	+0.34	+0.20	0.285
50172.6726	+107.33	-77.74	+0.81	+1.34	0.049
50210.5475	-72.88	+110.59	+0.34	-0.52	0.448
50415.9449	-19.56	+51.74	-1.09	-1.44	0.690
50443.8622	+61.84	-31.77	+0.24	-0.22	0.829
50461.8212	-7.76	+40.91	+0.13	-1.07	0.709
50492.7665	+65.14	-37.50	-1.62	-0.49	0.839
50523.7332	+110.43	-81.84	+0.49	+0.86	0.977
50550.6031	+29.55	+0.93	-0.86	-0.53	0.774
50782.9290	+61.52	-34.23	-1.17	-1.53	0.832

Table 4—Continued

HJD (2,400,000+)	RV_A (km s^{-1})	RV_B (km s^{-1})	$(O-C)_A$ (km s^{-1})	$(O-C)_B$ (km s^{-1})	Orbital Phase ^a
50824.0181	-2.19	+36.97	+0.98	-0.02	0.283
50857.7433	-24.68	+63.67	+1.31	+2.53	0.324
50887.7690	+70.36	-39.84	+0.15	+0.82	0.154
50917.5583	+96.28	-64.99	+1.45	+1.72	0.906
50953.5649	-17.45	+50.84	-0.92	-0.29	0.693
51109.9082	+84.51	-53.79	+0.70	+1.26	0.876
51157.9269	-62.04	+98.46	-0.69	-0.09	0.597
51196.8030	-26.74	+61.30	-0.87	+0.29	0.324
51243.6357	-35.85	+70.90	+0.71	-1.42	0.656
51274.6062	+42.49	-10.43	+0.06	+0.83	0.794
51310.5640	-69.93	+109.24	+0.24	+1.36	0.566
51492.8832	+13.86	+20.11	-0.71	+1.90	0.253
51540.8433	+107.12	-79.93	+0.15	-0.37	0.954
51573.7553	+3.04	+27.58	-0.57	-2.24	0.729
51603.7103	-76.74	+113.70	-0.80	-0.29	0.535
51633.5978	-24.22	+59.30	-0.59	+0.66	0.319

^aReferred to the time of maximum primary velocity, T_{max} .

Table 5. Spectroscopic orbital solution for HIP 48273.

Parameter	Value
Adjusted quantities	
P (days)	$3.05459836 \pm 0.00000084$
γ (km s^{-1})	$+16.342 \pm 0.066$
K_A (km s^{-1})	94.57 ± 0.12
K_B (km s^{-1})	100.07 ± 0.17
e	0 (fixed)
T_{max} (HJD-2,400,000) ^a	48419.18450 ± 0.00045
Derived quantities	
$M_A \sin^3 i$ (M_\odot)	1.1998 ± 0.0044
$M_B \sin^3 i$ (M_\odot)	1.1338 ± 0.0035
$q \equiv M_B/M_A$	0.9450 ± 0.0020
$a_A \sin i$ (10^6 km)	3.9722 ± 0.0051
$a_B \sin i$ (10^6 km)	4.2032 ± 0.0072
$a \sin i$ (R_\odot)	11.746 ± 0.013
Other quantities pertaining to the fit	
N_{obs}	112
Time span (days)	5816
σ_A (km s^{-1})	0.85
σ_B (km s^{-1})	1.21

^aTime of maximum primary velocity.

Table 6. Radial velocity measurements of TYC 6604-0118-1 (converted to the heliocentric frame) and residuals from the orbital solution.

HJD (2,400,000+)	RV_A (km s^{-1})	RV_B (km s^{-1})	$(O-C)_A$ (km s^{-1})	$(O-C)_B$ (km s^{-1})	Orbital Phase ^a
47554.7720	-7.62	+63.36	-1.33	-1.15	0.670
47569.8024	+64.02	-20.64	-1.74	-4.35	0.845
47575.7061	+92.66	-46.42	+0.67	-0.72	0.056
47587.6664	-38.88	+99.61	-1.84	+0.62	0.561
47612.6009	+76.99	-28.94	+0.22	-0.31	0.122
47640.5398	+0.12	+55.52	+1.61	-3.61	0.318
47642.5343	-25.94	+94.36	+3.53	+3.86	0.403
47643.5696	+92.82	-48.33	-1.74	+0.26	0.966
47669.6345	+70.91	-18.79	+0.53	+2.68	0.142
47670.6234	-4.20	+58.84	-1.88	-1.22	0.680
47671.6378	+35.20	+20.26	+0.21	+2.05	0.232
47672.6253	+38.23	+14.92	+2.99	-3.02	0.769
47693.6434	+47.84	-0.09	-0.45	-3.39	0.200
47872.8826	+2.74	+54.47	+2.47	-2.69	0.687
47874.8948	+39.40	+9.66	-1.03	-2.45	0.781
47875.8880	-0.55	+57.98	+2.22	-2.59	0.321
47877.8919	-30.13	+89.07	+1.35	-3.68	0.411
47879.8682	-42.34	+109.32	-0.62	+5.08	0.486
47881.8550	-37.11	+97.92	-1.07	+0.05	0.567
47894.8554	-20.18	+78.16	-2.34	+0.70	0.637
47895.8256	+61.08	-10.04	-1.17	+2.31	0.165
47900.8383	+79.57	-35.94	-1.10	-2.93	0.891
47923.7963	-22.54	+84.34	+0.11	+1.48	0.378
47940.7763	-23.84	+84.81	+1.41	-0.96	0.613
47942.7103	-7.61	+64.14	+0.45	-2.35	0.665
47957.6613	+48.35	+4.72	+1.28	+0.05	0.797
47958.6051	+2.08	+57.59	+0.44	+1.97	0.310
48305.7417	+80.32	-27.65	+1.08	+3.76	0.114
48351.6267	+91.84	-41.55	+2.28	+1.43	0.070
48669.8156	+72.79	-27.47	-1.73	-1.36	0.130
48675.8986	-37.78	+98.59	-0.97	-0.15	0.438
48693.8174	+55.63	-2.82	+0.65	+1.38	0.184
48696.6302	+8.55	+44.29	-2.91	-0.32	0.714
48711.5907	+69.54	-16.18	+1.67	+2.47	0.851

^aReferred to the time of maximum primary velocity, T_{max} .

Table 7. Spectroscopic orbital solution for
TYC 6604-0118-1.

Parameter	Value
Adjusted quantities	
P (days)	1.8386109 ± 0.0000065
γ (km s^{-1})	$+27.08 \pm 0.24$
K_A (km s^{-1})	69.07 ± 0.45
K_B (km s^{-1})	77.46 ± 0.66
e	0 (fixed)
T_{max} (HJD-2,400,000) ^a	47930.4559 ± 0.0013
Derived quantities	
$M_A \sin^3 i$ (M_\odot)	0.3168 ± 0.0061
$M_B \sin^3 i$ (M_\odot)	0.2825 ± 0.0046
$q \equiv M_B/M_A$	0.8917 ± 0.0099
$a_A \sin i$ (10^6 km)	1.746 ± 0.012
$a_B \sin i$ (10^6 km)	1.958 ± 0.017
$a \sin i$ (R_\odot)	5.323 ± 0.030
Other quantities pertaining to the fit	
N_{obs}	34
Time span (days)	1157
σ_A (km s^{-1})	1.68
σ_B (km s^{-1})	2.49

^aTime of maximum primary velocity.

Table 8. Radial velocity measurements of RXJ1100.0–3813 (converted to the heliocentric frame) and residuals from the orbital solution.

HJD (2,400,000+)	RV (km s ⁻¹)	ϵ^a (km s ⁻¹)	(O–C) (km s ⁻¹)	Orbital Phase ^b
50800.0147	+15.29	1.38	+2.17	0.811
50820.9981	+30.55	1.01	+2.98	0.090
50916.7760	+12.34	0.98	–4.81	0.834
51177.0529	–19.57	1.69	–1.32	0.362
51185.0599	+11.81	1.61	–0.64	0.193
51233.8754	+2.02	2.27	+2.36	0.739
51238.8837	–15.13	2.69	+6.40	0.386
51273.7667	+9.85	1.62	+0.99	0.788
51292.7421	–26.70	2.27	–4.13	0.605
51326.6527	–13.47	2.02	–6.02	0.298
51592.9498	+8.40	1.39	–0.86	0.210
51595.9099	–20.02	1.80	–1.28	0.366
51620.8570	–25.72	2.51	+2.69	0.532
51621.8438	–0.29	1.19	–1.91	0.250
51682.6914	–27.58	0.95	–0.61	0.558
51916.9919	+18.07	1.74	+1.82	0.171
51919.9880	–14.99	2.51	+1.85	0.353
51920.9792	+31.05	1.44	+1.99	0.075
51944.9736	–27.53	3.31	+0.15	0.547
52008.7316	+30.21	2.48	–1.79	0.974

^aInternal error.

^bReferred to the time of maximum primary velocity, T_{\max} .

Table 9. Spectroscopic orbital solution for
RXJ1100.0–3813.

Parameter	Value
Adjusted quantities	
P (days)	1.373286 ± 0.000031
γ (km s ⁻¹)	$+1.69 \pm 0.82$
K_A (km s ⁻¹)	30.7 ± 1.1
e	0 (fixed)
T_{\max} (HJD–2,400,000) ^a	51453.9590 ± 0.0074
Derived quantities	
$a_A \sin i$ (10 ⁶ km)	0.58 ± 0.16
$f(M)$ (M _⊙)	0.0041 ± 0.0034
$M_B \sin i$ (M _⊙)	$0.1603 (M_A + M_B)^{2/3}$
Other quantities pertaining to the fit	
N_{obs}	20
Time span (days)	1209
σ_{RV} (km s ⁻¹)	3.23

^aTime of maximum primary velocity.

Table 10. Radial velocity measurements of HD 97131 (converted to the heliocentric frame) and residuals from the orbital solution.

HJD (2,400,000+)	RV _A (km s ⁻¹)	RV _{Ba} (km s ⁻¹)	(O-C) _A (km s ⁻¹)	(O-C) _{Ba} (km s ⁻¹)	Orbital Phase ^a	Orbital Phase ^b	Δt^c (days)
50444.0088	-38.08	-1.69	+0.69	+0.69	0.422	0.819	+0.0006
50768.0287	-10.13	-38.13	-1.33	-2.72	0.849	0.766	+0.0002
50772.0430	-9.54	+2.06	-1.39	+3.87	0.879	0.045	+0.0000
50799.0388	-28.57	-52.77	+0.16	+0.40	0.081	0.371	-0.0007
50820.9887	-42.30	+3.13	-0.02	+0.54	0.246	0.832	-0.0002
50821.9875	-42.03	-49.32	+0.38	-0.70	0.253	0.399	-0.0001
50822.9702	-42.59	+21.17	-0.08	-0.32	0.261	0.957	-0.0001
50823.9700	-42.50	-56.75	+0.07	-0.91	0.268	0.524	-0.0001
50826.9366	-42.37	-6.39	+0.23	-0.05	0.290	0.208	+0.0000
50827.9684	-41.99	-5.73	+0.56	+0.09	0.298	0.794	+0.0001
50829.9656	-42.09	+18.36	+0.30	-0.53	0.313	0.928	+0.0001
50851.7785	-33.77	-39.01	+2.06	-2.88	0.476	0.311	+0.0008
50853.7782	-36.98	-56.01	-2.07	+3.26	0.491	0.446	+0.0008
50861.9068	-31.24	+12.04	-0.43	-0.11	0.552	0.061	+0.0009
50867.7702	-29.15	-58.43	-1.63	-1.06	0.596	0.390	+0.0009
50871.7422	-23.81	-51.45	+1.36	+1.25	0.626	0.644	+0.0009
50884.8500	-16.25	-0.24	+0.80	-0.34	0.724	0.086	+0.0008
50916.7468	-12.11	-23.49	-0.19	+0.05	0.963	0.194	-0.0004
51177.0224	-6.63	-5.12	+1.93	-3.42	0.912	0.953	-0.0002
51179.0602	-8.92	-9.34	+0.29	-0.84	0.928	0.109	-0.0002
51185.0151	-12.63	-75.81	+0.27	+0.44	0.972	0.490	-0.0005
51185.9845	-13.59	+3.10	+0.14	+0.81	0.979	0.040	-0.0005
51187.0145	-14.61	-63.22	+0.07	+0.32	0.987	0.625	-0.0005
51233.8649	-40.84	-10.56	+1.06	-0.32	0.338	0.222	+0.0003
51235.8679	-42.42	-41.03	-0.92	+1.51	0.353	0.359	+0.0003
51236.8613	-41.85	+17.13	-0.58	-0.51	0.361	0.923	+0.0004
51237.8970	-40.93	-57.51	+0.09	-0.26	0.368	0.511	+0.0004
51238.8630	-41.28	+18.74	-0.52	-0.28	0.376	0.060	+0.0004
51239.8435	-39.17	-48.74	+1.32	-1.19	0.383	0.616	+0.0005
51240.8838	-39.48	-8.46	+0.70	-0.76	0.391	0.207	+0.0005
51241.8516	-43.12	-16.51	-3.24	+0.32	0.398	0.756	+0.0005
51267.7662	-28.07	-65.08	-0.23	+0.39	0.592	0.468	+0.0009
51268.7760	-27.54	+11.47	-0.29	+0.16	0.600	0.041	+0.0009
51269.7769	-26.93	-58.88	-0.27	-0.95	0.607	0.609	+0.0009
51271.7718	-24.43	-31.13	+1.05	-1.09	0.622	0.742	+0.0009
51272.7534	-23.23	-41.82	+1.66	-1.03	0.629	0.299	+0.0009
51273.7540	-24.03	+0.27	+0.25	+2.51	0.637	0.867	+0.0009
51274.7941	-22.97	-67.12	+0.67	+0.60	0.645	0.458	+0.0009
51292.7553	-13.36	-59.67	-0.62	-0.53	0.779	0.654	+0.0006
51325.6966	-20.26	-56.37	-0.06	-0.34	0.026	0.355	-0.0006

^aReferred to the time of periastron passage in the outer orbit.

^bReferred to the time of maximum primary velocity in the inner orbit.

^cCorrection for light travel time.

Table 11. Spectroscopic orbital solution for HD 97131.

Parameter	Value
Adjusted quantities in outer orbit (A–B)	
P_{AB} (days)	133.51 ± 0.20
γ (km s^{-1})	-27.09 ± 0.15
K_A (km s^{-1})	17.24 ± 0.29
K_B (km s^{-1})	11.64 ± 0.35
e_{AB}	0.191 ± 0.016
ω_A (deg)	58.6 ± 4.3
T (HJD–2,400,000) ^a	51453.9590 ± 0.0074
Derived quantities in outer orbit (A–B)	
$a_A \sin i$ (10^6 km)	31.08 ± 0.52
$a_B \sin i$ (10^6 km)	20.98 ± 0.66
$a_{AB} \sin i$ (R_\odot)	74.8 ± 1.3
$M_A \sin i$ (M_\odot)	0.1271 ± 0.0079
$M_B \sin i$ (M_\odot)	0.1883 ± 0.0088
$q \equiv M_B/M_A$	1.481 ± 0.051
Adjusted quantities in inner orbit (Ba–Bb)	
P_B (days)	1.761488 ± 0.000020
K_{Ba} (km s^{-1})	39.66 ± 0.33
e_B	0 (fixed)
T_{\max} (HJD–2,400,000) ^b	51044.9943 ± 0.0024
Derived quantities in inner orbit (Ba–Bb)	
$a_{Ba} \sin i$ (10^6 km)	0.9605 ± 0.0087
$f(M)$ (M_\odot)	0.01138 ± 0.00031
$M_{Bb} \sin i$ (M_\odot)	$0.2249 (M_{Ba} + M_{Bb})^{2/3}$
Other quantities pertaining to the fit	
N_{obs}	40
Time span (days)	882
σ_A (km s^{-1})	1.11
σ_{Ba} (km s^{-1})	1.47

^aTime of periastron passage.

^bTime of maximum primary velocity.

Table 12. Radial velocity measurements of RXJ1115.1–3233 (converted to the heliocentric frame) and residuals from the orbital solution.

HJD (2,400,000+)	RV _A (km s ⁻¹)	RV _B (km s ⁻¹)	(O–C) _A (km s ⁻¹)	(O–C) _B (km s ⁻¹)	Orbital Phase ^a
50800.0462	+33.56	–61.33	+1.50	–1.74	0.824
50821.0455	+2.49	+9.75	+2.59	+26.05	0.237
50884.8566	+38.29	–85.97	–1.55	–15.91	0.841
50916.7556	+47.34	–89.46	–1.13	–7.77	0.140
51177.0286	+25.40	–57.81	+1.74	–9.52	0.808
51185.0241	–73.92	+85.24	+0.44	+1.55	0.392
51187.0223	–29.69	+20.21	–2.59	+0.16	0.287
51233.8874	–29.20	+17.92	+1.79	–7.37	0.295
51235.8818	+25.68	–47.76	+0.03	+3.20	0.189
51238.8703	–91.80	+98.68	+0.59	–9.28	0.528
51272.7801	–19.62	–9.80	–0.84	–18.66	0.728
51273.7814	+31.16	–63.32	–0.17	–4.71	0.177
51292.7703	–40.55	+30.12	–1.09	–6.57	0.689
51325.7099	–89.40	+110.93	+0.79	+5.94	0.454
51540.0251	–94.15	+101.37	–1.19	–7.36	0.521

^aReferred to the time of maximum primary velocity, T_{\max} .

Table 13. Spectroscopic orbital solution for
RXJ1115.1–3233.

Parameter	Value
Adjusted quantities	
P (days)	2.230887 ± 0.000024
γ (km s ⁻¹)	-7.00 ± 0.41
K_A (km s ⁻¹)	86.75 ± 0.71
K_B (km s ⁻¹)	116.8 ± 5.2
e	0 (fixed)
T_{\max} (HJD–2,400,000) ^a	51137.3021 ± 0.0020
Derived quantities	
$M_A \sin^3 i$ (M _⊙)	1.12 ± 0.12
$M_B \sin^3 i$ (M _⊙)	0.831 ± 0.049
$q \equiv M_B/M_A$	0.743 ± 0.037
$a_A \sin i$ (10 ⁶ km)	2.661 ± 0.024
$a_B \sin i$ (10 ⁶ km)	3.58 ± 0.18
$a \sin i$ (R _⊙)	8.97 ± 0.25
Other quantities pertaining to the fit	
N_{obs}	15
Time span (days)	740
σ_A (km s ⁻¹)	1.55
σ_B (km s ⁻¹)	11.8

^aTime of maximum primary velocity.

Table 14. Radial velocity measurements
(converted to the heliocentric frame) for
stars without orbital solutions.

HJD (2,400,000+)	RV (km s ⁻¹)	ϵ^a (km s ⁻¹)
HIP 50796		
46422.9750.....	+16.31	0.22
46537.6905.....	+14.06	0.41
46540.7560.....	+12.68	0.29
46569.7043.....	+12.02	0.52
52391.6615.....	+47.98	0.60
52395.7197.....	+48.09	0.42
52419.6668.....	+40.40	0.49
52421.6565.....	+40.59	0.35
52423.6634.....	+40.47	0.42
52424.6403.....	+41.03	0.49
HIP 53486		
48725.6069.....	+4.78	0.36
48966.8844.....	+5.25	0.32
49025.7618.....	+6.28	0.48
49756.8749.....	+6.33	0.29
51492.9060.....	+5.85	0.42
51530.9207.....	+4.72	0.64
52038.3739 ^b	+5.08	0.11
HD 95490		
50772.0382.....	-7.18	0.44
50800.0195.....	-7.80	0.44
50827.9896.....	-7.27	0.50
50861.9139.....	-7.80	0.52
TW Hya		
50770.0392.....	+13.07	0.71
50800.0243.....	+12.15	0.64
50821.0353.....	+12.65	0.64
50823.0035.....	+13.44	0.68
50828.9781.....	+13.27	0.58
51260.4821 ^c	+12.45	0.40
51331.5619 ^c	+11.57	0.40

Table 14—Continued

HJD (2,400,000+)	RV (km s ⁻¹)	ϵ^a (km s ⁻¹)
51622.5972 ^c	+12.65	0.40
TWA-2A		
50772.0306.....	+11.39	0.49
50800.0321.....	+11.46	0.56
50827.9935.....	+11.02	0.57
51273.7911.....	+10.84	0.59
51294.7732.....	+10.22	0.81
51326.6672.....	+10.87	0.71
51331.5720 ^c	+10.90	0.30
51621.5524 ^c	+11.25	0.30
51625.5868 ^c	+10.80	0.30
RXJ1109.7–3907		
50771.0438.....	+5.03	1.27
50799.0455.....	–1.52	1.03
50821.0075.....	–3.45	1.20
50828.9511.....	–3.17	1.17
51185.0518.....	–1.81	0.99
51236.8875.....	–2.69	1.29
51237.9027.....	–2.02	1.28
CD–37°7097		
50799.0422.....	–7.92	0.73
50821.0125.....	–7.95	0.85
51236.8674.....	–8.71	0.76
TWA-12		
50822.9923.....	+13.62	0.78
50828.9678.....	+12.12	0.72
52034.7186.....	+4.13	2.19
52038.7208.....	+14.47	3.26
TWA-13A		
50769.0345.....	+11.81	1.13
50799.0620.....	+13.23	1.18
50827.9841.....	+11.54	0.90

Table 14—Continued

HJD (2,400,000+)	RV (km s ⁻¹)	ϵ^a (km s ⁻¹)
51236.8959	+10.11	1.01
TWA-13B		
50770.0257	+13.69	1.03
50799.0585	+12.94	0.77
50827.9764	+12.31	1.04
51236.9068	+11.33	1.09
TWA-9A		
51233.8946	+9.87	0.70
51238.9328	+11.14	0.64
51271.7821	+8.88	0.74
51294.7997	+8.97	0.76
51326.7001	+10.24	0.88
51597.9406	+11.56	0.48
51620.8847	+9.20	0.61
51653.7926	+8.16	1.05
51683.7382	+10.92	1.09
51917.0362	+10.64	0.52
51943.9794	+11.42	0.71
52009.7888	+6.14	0.86
52034.7695	+7.09	1.03
52035.7202	+8.29	0.87
52037.7009	+7.68	1.06
52274.0472	+11.90	0.94
52336.8759	+9.18	0.62
52360.8108	+8.97	0.59

^aInternal error.

^bMeasurement from Tautenburg.

^cMeasurement from La Silla (FEROS).

Table 15. Summary of radial velocity results for our sample.

TWA #	Other names	N_{obs}	Mean CfA RV (km s^{-1})	Other RVs ^a (km s^{-1})	Remarks
1	HIP 48273	112	$+16.342 \pm 0.066$	+17.0, +17.4	Double-lined binary (orbit)
2	TYC 6604-0118-1	34	$+27.08 \pm 0.24$	-19, +54	Double-lined binary (orbit)
3	HIP 50796	10	...	+22.4	Variable RV
4	HIP 53486	7	$+5.47 \pm 0.26$	+4.3	
5	RXJ1100.0-3813	20	$+1.69 \pm 0.82$		Single-lined binary (orbit)
6	HD 95490	4	-7.51 ± 0.17		
7	TWA-1 TW Hya	8	$+12.66 \pm 0.22$	+12, +12.5, +13.5, +13	
8	TWA-2A CD-29°8887A	9	$+10.97 \pm 0.12$	+9.7, +10, +12	
9	RXJ1109.7-3907	7	-1.4 ± 1.1:	-2.0	Variable RV?
10	TWA-3A Hen 3-600A	47	...	+10.4, +12	Double-lined?
11	HD 97131	40	-27.09 ± 0.15		Double-lined triple (orbit)
12	CD-37°7097	3	-8.19 ± 0.26		
13	RXJ1115.1-3233	15	-7.00 ± 0.41		Double-lined binary (orbit)
14	TWA-12 RXJ1121.1-3845	4	+11.1 ± 2.4:	+10.9	Variable RV?
15	TWA-13A RXJ1121.3-3447N	4	$+11.67 \pm 0.64$	+10.5, +11.3	
16	TWA-13B RXJ1121.3-3447S	4	$+12.57 \pm 0.50$	+12.0, +11.6	
17	TWA-4A HD 98800A	152	$+12.75 \pm 0.10$		Double-lined binary (orbit)
18	TWA-4B HD 98800B	152	$+5.73 \pm 0.14$		Double-lined binary (orbit)
19	TWA-5A CD-33°7795A	54	...	+14, -30.6	Double-lined?
20	TWA-9A CD-36°7429A	18	$+9.46 \pm 0.38$:		Variable RV?
Radial velocity measurements for other members of the TW Hya association not in our sample					
...	TWA-3B Hen 3-600B	$+14.0 \pm 0.4$	
...	TWA-7 TYC 7190-2111-1	$+11.80 \pm 0.29$	
...	TWA-8A RXJ1132.7-2651	+7.5	
...	TWA-11A HR 4796A	$+9.4 \pm 2.3$	
...	TWA-11B HR 4796B	$+9 \pm 1$	
...	TWA-19A HD 102458	$+11.5 \pm 3.8$	

^aMeasurements by Popper & Shajn (1948), Mayor & Mazeh (1987), de la Reza et al. (1989), Stauffer et al. (1995), Reipurth, Pedrosa & Lago (1996), Sterzik et al. (1999), Torres et al. (2000), Barbier-Brossat & Figon (2000), Neuhäuser et al. (2000b), and Song et al. (2002).

Table 16. Members and candidate members from the kinematic study by Makarov & Fabricius (2001) with measured radial velocities.

TWA #	Other names	μ (mas yr ⁻¹)	D_{kin} (pc)	D_{trig} (pc)	RV_{pred} (km s ⁻¹)	RV_{obs} (km s ⁻¹)
Objects with velocities reported in this paper						
1	HIP 48273	157.9	26.6	45.9	+10.7	+16.3
2	TYC 6604-0118-1	63.7	62.8	...	+16.5	+27.1
3	HIP 50796	79.1	53.8	34.0	+13.1	...
4	HIP 53486	268.1	16.7	17.6	+3.7	+5.5
7	TWA-1 TW Hya	75.4	57.1	56.4	+12.7	+12.7
8	TWA-2A CD-29°8887A	92.6	47.1	...	+10.6	+11.0
17/18	TWA-4A/B HD 98800A/B	96.8	45.7	46.7	+9.1	+9.2
19	TWA-5A CD-33°7795A	86.7	50.9	...	+10.0	...
20	TWA-9A CD-36°7429A	58.1	76.3	50.3	+12.6	+9.5:
Members with velocities from other sources						
...	TWA-7 TYC 7190-2111-1	125.7	33.6	...	+11.0	+11.8
...	TWA-11A/B HR 4796A/B	57.4	78.1	67.1	+10.5	+9.2
...	TWA-19A HD 102458A	34.9	125.5	104.0	+20.0	+11.5

Table 17. Objects currently considered members of the TW Hya association.

Other name		R.A. ^a (J2000)	Dec. ^a (J2000)	SpT	V ^b (mag)	B−V (mag)	μ_{α}^a (mas yr ^{−1})	μ_{δ}^a (mas yr ^{−1})	π_{HIP} (mas)	Li I λ 6708 eq. width (Å)	Mean RV (km s ^{−1})
TWA-1	TW Hya	11:01:51.9	−34:42:17	K7e	10.92	0.97	−73.4	−17.5	17.72	0.426	+12.66 ± 0.22
TWA-2A	CD−29° 8887A	11:09:13.8	−30:01:40	M2e	11.07	1.42	−90.1	−21.1	...	0.494	+10.97 ± 0.12
TWA-2B	CD−29° 8887B	+0′′3	+0′′5	M2	+0.81K
TWA-3A	Hen 3-600A	11:10:28.0	−37:31:52	M3e	12.04	1.52	−96.5	+16.3	...	0.563	+11.2
TWA-3B	Hen 3-600B	−0′′8	−1′′2	M3.5	+0.52K	0.52	+14.0
TWA-4A	HD 98800A	11:22:05.3	−24:46:40	K4-5	9.41	1.15	−91.7	−31.1	21.43	0.425	+12.75 ± 0.10
TWA-4B	HD 98800B	+0′′0	+0′′8	K7+M1	9.94	1.28	0.335+0.450	+5.73 ± 0.14
TWA-5A ^c	CD−33° 7795A	11:31:55.3	−34:36:27	M1.5	11.54	1.48	−81.6	−29.4	...	0.572	...
TWA-5B	CD−33° 7795B	−0′′1	+2′′0	M8.5	+4.6K
TWA-6	TYC 7183-1477-1	10:18:28.7	−31:50:03	K7	11.62	1.31	−57.0	−20.6	...	0.56	...
TWA-7	TYC 7190-2111-1	10:42:30.1	−33:40:17	M1	11.65	1.46	−122.2	−29.3	...	0.44	+11.80 ± 0.29
TWA-8A	RXJ1132.7−2651	11:32:41.3	−26:51:56	M2	12.23	...	−99.0	−38.0	...	0.53	+7.5
TWA-8B		−1′′3	−13′′0	M5	+1.57K	0.56	...
TWA-9A	CD−36° 7429A	11:48:24.2	−37:28:49	K5	11.26	1.26	−55.4	−17.7	19.87	0.47	+9.46 ± 0.38:
TWA-9B		−5′′7	+0′′8	M1	14.00	1.43	0.48	...
TWA-10	1RXS J123504.4−413629	12:35:04.2	−41:36:39	M2.5	12.96	1.43	−69.2	−37.6	...	0.46	...
TWA-11A	HR 4796A	12:36:01.0	−39:52:10	A0	5.78	0.00	−53.3	−21.2	14.91	...	+9.4 ± 2.3
TWA-11B	HR 4796B	−5′′0	−4′′7	M2.5	13.3	0.55	+9 ± 1
TWA-12	RXJ1121.1−3845	11:21:05.5	−38:45:17	M2	12.85	...	−38.3	−10.7	...	0.530	+11.1 ± 2.4:
TWA-13A	RXJ1121.3−3447S	11:21:17.5	−34:46:51	M1e	11.46	0.570	+12.57 ± 0.50
TWA-13B	RXJ1121.3−3447N	−2′′8	+4′′3	M2e	12.00	0.650	+11.67 ± 0.64
TWA-14	1RXS J111325.1−452344	11:13:26.2	−45:23:43	M0	11.85R	...	−42.3	−6.0	...	0.60	...
TWA-15A	1RXS J123420.1−481514	12:34:20.7	−48:15:15	M1.5	13.51R	0.65	...
TWA-15B		−1′′0	−5′′0	M2	−0.10R ^d	0.54	...
TWA-16 ^e	1RXSJ123456.1−453808	12:34:56.3	−45:38:08	M1.5	11.64R	...	−40.0	−12.2	...	0.36	...
TWA-17	1RXS J132046.5−461139	13:20:45.4	−46:11:38	K5	11.69R	...	−20.0	−3.7	...	0.49	...
TWA-18	1RXS J132137.0−442133	13:21:37.2	−44:21:52	M0.5	12.08R	...	−42.4	−29.2	...	0.42	...
TWA-19A	HD 102458	11:47:24.5	−49:53:03	G5	9.14	0.63	−33.7	−9.1	9.62	0.19	+11.5 ± 3.8
TWA-19B	1RXS J114724.3−495250	−37′′8	−1′′3	K7	11.06R	...	−34.9	−7.6	...	0.40	...
Other candidate members from recent studies											
...	2MASSW J1207334−393254	12:07:33.4	−39:32:54	M8	11.96K	...	−100 ^f	−30 ^f	...	0.30	...
...	TYC 7760-0835-1	12:13:07.0	−40:56:32	...	9.81	0.51	−30.8	−10.9	...	0.161	+10.0 ± 2.6
...	TYC 8238-1462-1	12:21:55.7	−49:46:12	...	10.02	0.76	−37.4	−14.2	...	0.294	+12.0 ± 3.0
...	TYC 8234-2856-1	12:22:04.3	−48:41:25	...	10.50	0.82	−30.0	−12.1	...	0.161	+13.2 ± 2.4

^aPositions (epoch 2000) and proper motions are taken preferentially from the Tycho-2 catalog (Høg et al. 2000) or from the UCAC1 catalog (Zacharias et al. 2000), when available.

^bMagnitudes or magnitude differences available only in the *R* or *K* bands, instead of *V*, are labeled.

^cClose visual binary with a separation of 0′′0548 and a magnitude difference $\Delta H = 0.09$ (Macintosh et al. 2001).

^dAlthough formally the magnitude difference indicates a brighter secondary (Zuckerman et al. 2001b), measurement errors in both the magnitudes and spectral types suggest the stars are indistinguishable within the errors (Schwartz & Zuckerman 2002, priv. comm.).

^eClose visual binary with a separation of 0′′67 and a brightness ratio ~ 0.9 in *H* (see Zuckerman et al. 2001b).

^fProper motions relative to other stars in the field (Gizis 2002).